

**Iterated Timing Analysis and SPLICE1**

**by**

**Resve A. Saleh**

**June 1983**

**Electronics Research Laboratory**

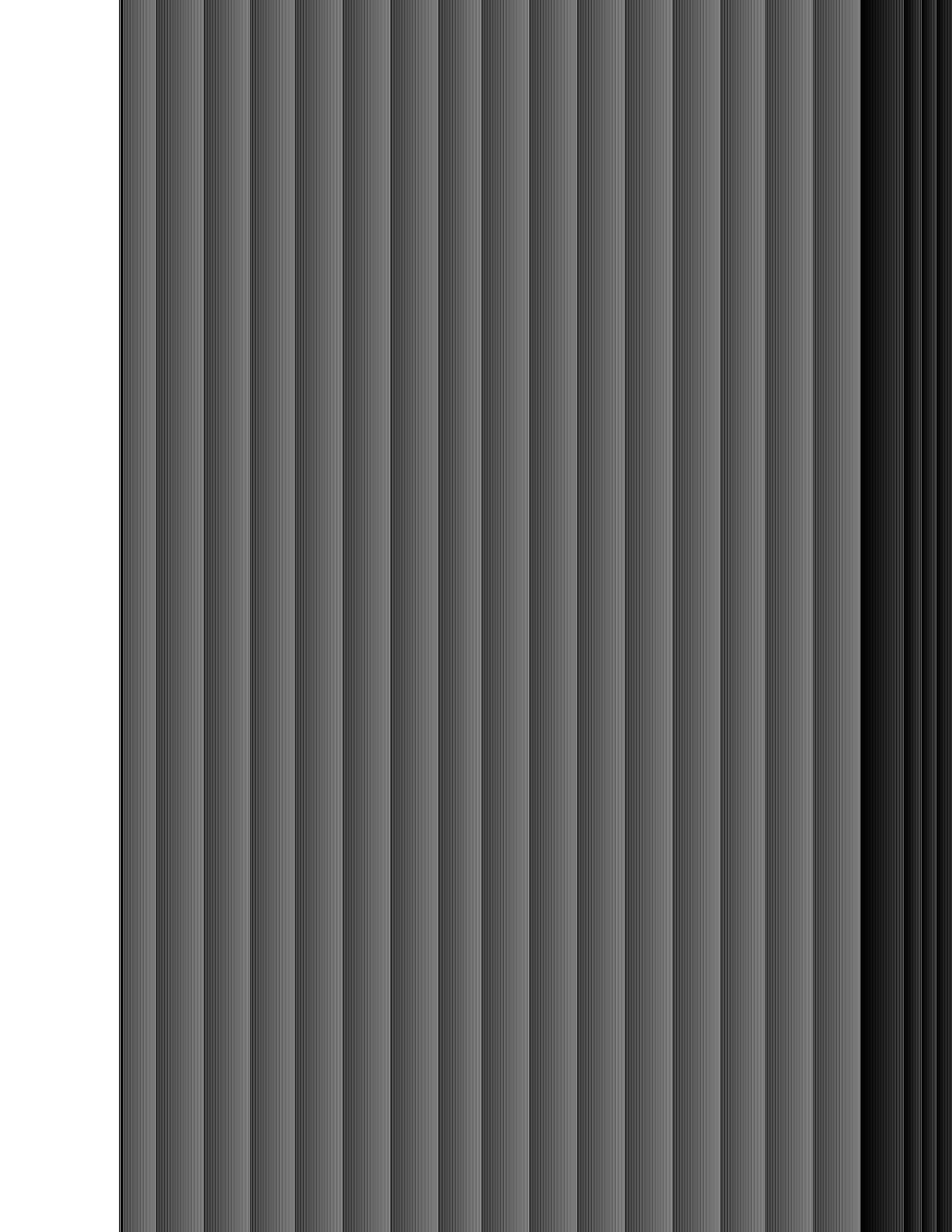
**University of California**

**Berkeley, California. 94720**

### **Abstract**

SPLICE1 is a mixed-mode simulation program for large-scale integrated circuits. It performs concurrent electrical and logic simulation using event-driven selective-trace techniques. The electrical analysis uses a new algorithm, called Iterated Timing Analysis (ITA), which performs accurate electrical waveform analysis much faster than SPICE2. The logic analysis features a new MOS-oriented state model and a fanout dependent delay model, and handles bidirectional transfer gates in a consistent manner.

This report describes the new algorithms and the details of the implementation in SPLICE1.6. Program performance characteristics and a number of simulation results are also included.



## **Acknowledgements**

I would like to express my appreciation to my research advisor Prof. A. Richard Newton for his patience, encouragement and guidance throughout course of this work. I would also like to thank Prof. Don O. Pederson and Prof. Alberto Sangiovanni-Vincentelli for their support.

I wish to thank everyone in the CAD group at Berkeley but a few people deserve special mention. In particular, I would like to thank Jim Klockner for the many long hours of help generating examples, fixing bugs and engaging in useful discussions. I am also grateful to Jacob White for the discussions on the theoretical aspects of the work.

I wish to acknowledge the assistance of Graeme Boyle, Steve Potter and Jack Hurt and convey my appreciation to Ian Getreu and John Crawford at Tektronix in Beaverton, Oregon. I would also like to send a special thanks to Mike Caughey and the ICCAD group at MITEL Corp. in Ottawa, Canada for their encouragement.

Finally, I wish to thank my wife, Lynn, and my family members for their continuing support.

This work was supported in part by NSERC (Natural Science and Engineering Research Council) of Canada, the Hewlett-Packard Company, Digital Equipment Corporation and Tektronix Corporation.



## TABLE OF CONTENTS

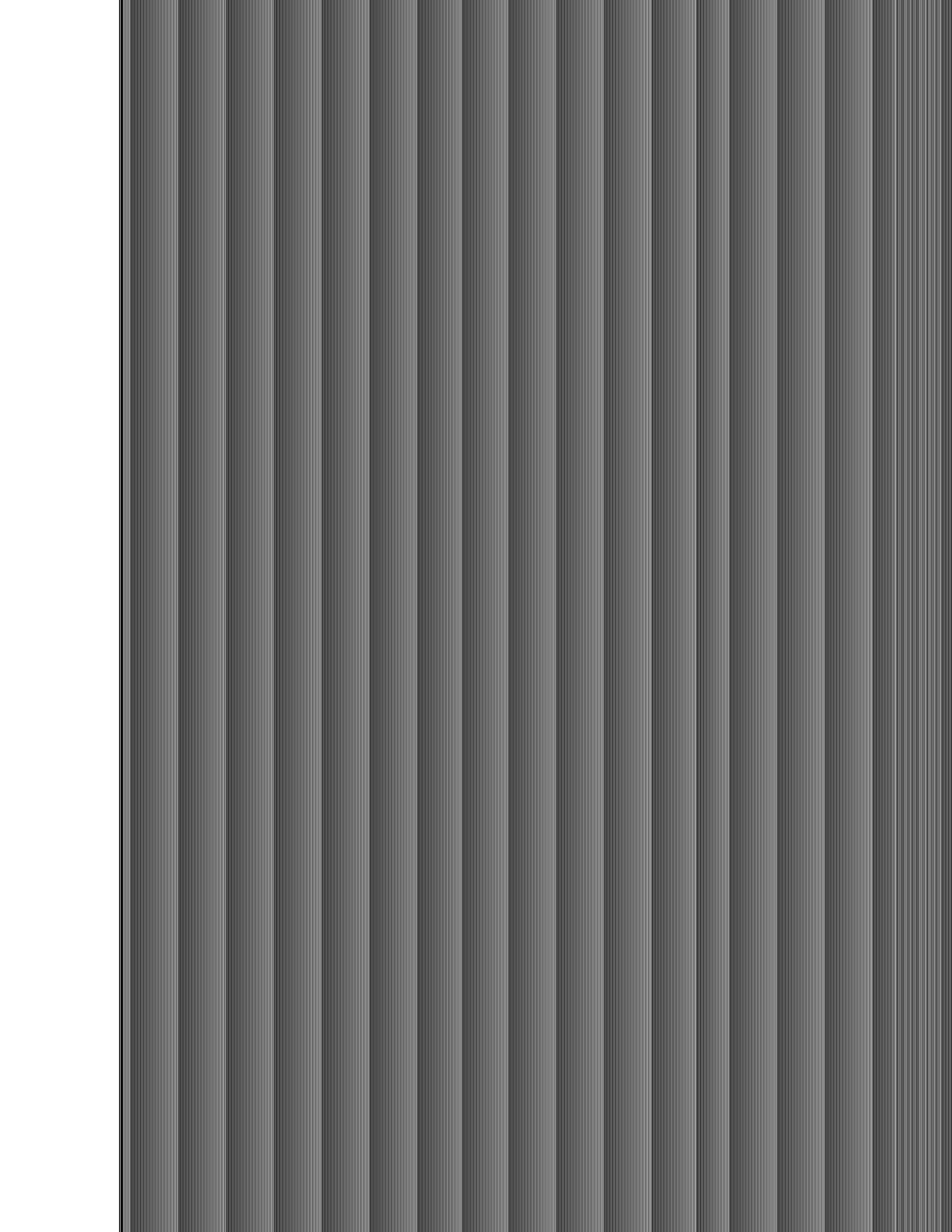
<b>CHAPTER 1: INTRODUCTION</b> .....	<b>1</b>
<b>CHAPTER 2: Iterated Timing Analysis</b> .....	<b>4</b>
2.1 Introduction.....	4
2.2 The Simulation Problem .....	4
2.3 Motivation for a New Simulation Approach.....	5
2.4 Relaxation-based Electrical Simulation.....	10
2.5 The ITA Algorithm .....	11
2.5.1 The Gauss-Seidel Iteration Method .....	11
2.5.2 A Non-linear Gauss-Seidel Iterative Approach .....	13
2.5.3 The SOR-Newton Iteration.....	15
2.5.4 Convergence of the SOR-Newton Iteration.....	16
2.6 Implementation in SPLICE.....	17
2.6.1 Program Flow.....	18
2.6.2 Details of Node Processing.....	18
2.6.3 Element Models.....	19
2.7 ITA Simulation Results.....	20
2.8 Optimizations in the Present Implementation .....	21
<b>CHAPTER 3: Enhancements to the Logic Analysis</b> .....	<b>23</b>
3.1 Introduction.....	23
3.2 The State Model .....	24
3.2.1 A MOS-oriented Logic Model.....	24
3.2.2 State Model Definition.....	25
3.2.3 Using the State Model.....	27
3.3 The Delay Model.....	27

3.3.1 Factors Affecting Switching Delay .....	27
3.3.2 Delay Model for Simple Gates .....	28
3.3.3 Delay Model for Multi-output Elements.....	29
3.3.4 Delay Models for Transfer Gates .....	30
3.3.5 Delay to an Unknown Value.....	32
3.4 Spike Handling.....	32
3.5 Transfer Gate Modeling Issues.....	35
3.5.1 Bidirectional Transfer Gates.....	35
3.5.2 Unknowns at Gate Inputs.....	36
3.5.3 Node Decay .....	38
3.6 Logic Simulation Implementation Details.....	39
3.6.1 General Program Flow .....	39
3.6.2 Node Processing Details.....	39
3.7 Switch-level Simulation .....	40
<b>CHAPTER 4: Examples and Results .....</b>	<b>42</b>
4.1 Program Performance Statistics.....	43
4.2 Profile Statistics .....	45
4.3 Factors Affecting Execution Time in Electrical Simulation .....	46
4.3.1 CPU-time vs. MRT.....	46
4.3.2 CPU-time vs. MINDVSCH.....	47
4.3.3 Effect of Floating Capacitors .....	48
4.3.4 CPU-time vs. SOR.....	49
4.4 SPICE2 vs. SPICE1.6.....	49
4.5 NMOS OpAmp Example.....	50
<b>CHAPTER 5: CONCLUSIONS .....</b>	<b>52</b>
 <b>REFERENCES</b>	

**APPENDIX I: SPLICE1.6 User's Guide**

**APPENDIX II: SPLICE1.6 Data Structures**

**APPENDIX III: SPLICE1.6 Electrical Model Equations**



## CHAPTER 1

### 1. INTRODUCTION

SPLICE1 is a *mixed-mode* simulation program for large digital MOS integrated circuits (IC). It performs time-domain transient analysis which tends to be the most time-consuming and memory-intensive task in simulation today. The enhancements made to the program are described in this report. The starting point for this work was SPLICE1.3[1]. This early version of SPLICE1 included 4-state logic simulation, simple timing analysis and a SPICE-like circuit simulation capability[1, 2].

While this version provided a degree of functionality, it suffered from modeling and accuracy problems intrinsic to the algorithms used in the program. Specifically, the 4-state logic model was not sufficient to perform an accurate true-value logic simulation of general MOS circuits containing transfer gates and wired connections (i.e., more than one gate controlling the state of a node). The simple timing analysis algorithm had inherent accuracy limitations and stability problems and had some difficulty handling circuits containing floating elements and tight feedback loops. These, and other issues, are examined in detail elsewhere[3] and will be elaborated further in later sections.

The latest version, SPLICE1.6, overcomes these problems by using state-of-the-art algorithms in place of previous ones.

The electrical analysis is performed using a new technique called *Iterated Timing Analysis* (ITA) which can be derived from simple timing analysis[4, 5]. In this approach the non-linear differential circuit equations are solved using a converged relaxation iteration instead of the direct matrix solution approach used in standard circuit simulators[6]. It is as accurate

as SPICE2, assuming identical device models, and has guaranteed convergence and stability properties. Due to the selective trace feature in SPLICE1, the execution time is up to two orders of magnitude faster than SPICE2 for comparable waveform accuracy. Another key feature of the ITA method is its ability to perform a transient analysis of complex analog circuits, as will be shown later. Iterated Timing Analysis has shown so much promise that efforts are being directed to generalize it as a standard technique for accurate electrical simulation. Therefore, a matrix-oriented simulation capability is no longer available in SPLICE1.

The logic analysis capabilities have also been extended to include the notion of multiple strengths or impedance levels [3] as is available in most modern MOS-oriented logic simulators[7,8,9,10] . While other simulators usually limit the number of strengths to three, there is no practical limit in SPLICE1.6, which allows up to  $2^{16} - 1$  levels. More than three strengths are often required to model the interaction between transfer gates of differing geometry[3] . The processing of the gates and nodes proceeds in a manner similar to the electrical analysis. In fact, the logic analysis may be thought of as a relaxation-based method in which the elements are represented by simple logic models rather than complex analytical equations. This concept, together with the idea of multiple impedance levels, allows for a more consistent signal representation and signal conversion in the mixed-mode environment. Clearly, there is a correspondence between an electrical voltage and the logic levels. With the notion of strengths, there is now a natural correspondence between the electrical output conductance of an element and the logic output strength of the element.

SPLICE1 can also be used to perform a switch-level simulation[9, 10] to verify circuit functionality at the transistor level. It handles CMOS, NMOS and PMOS circuits in both static and dynamic configurations. SPLICE1.6 currently performs unit-delay simulation of switch-level circuits.

Although SPLICE1 originally included a table look-up scheme to speed up MOS model evaluation[4, 5] it was subsequently dropped from the program. Research on optimal table models and structures is continuing in an independent effort [11] and this feature may be reinstated in a later version. Therefore, this report does not address the issue of table-driven MOS models.

The remainder of this report is divided into four chapters. In Chap. 2, the ITA algorithm is described in detail. The enhancements made to the logic analysis are presented in Chap. 3. Chap. 4 provides some insight into the new algorithms through the use of examples. Finally, in Chapter 5, the general conclusions are stated with specific mention of future directions.

## CHAPTER 2

### 2. Iterated Timing Analysis

#### 2.1. Introduction

A new form of electrical analysis, called *Iterated Timing Analysis* (ITA), is described in this chapter. The motivation for this work is presented using SPLICE1.3 as an example of Non-iterated Timing Analysis (NTA). A simple mathematical treatment of the ITA method is presented here although a complete mathematical analysis of relaxation-based methods, presented in a rigorous and unified framework, may be found in reference[12]. The details of the implementation in SPLICE1.6 are also included in this chapter.

#### 2.2. The Simulation Problem

The general circuit analysis problem in the time domain requires the solution of a set of non-linear Ordinary Differential Equations (ODE) of the form:

$$C(v,u)\dot{v} = -f(v,u) \quad (2-1)$$

This formulation can be derived by writing *Kirchoff's Current Law* (KCL) at every node except the ground node in a given circuit. A grounded capacitor,  $C(v,u)$ , is assumed to be present at each node, which introduces the differential operator into Eqn. (2-1). The simulation task is to determine the unknown voltages,  $v$ , for every node at every timepoint due to some input excitation,  $u(t)$ .

The technique used in SPICE2 to solve Eqn. (2-1) is to first convert the set differential equations into a set of algebraic, difference equations using a stiffly-stable integration formula[6] . Then the non-linear difference equations are converted to a set of linear equations of the form:

$$GV = I \quad (2-2)$$

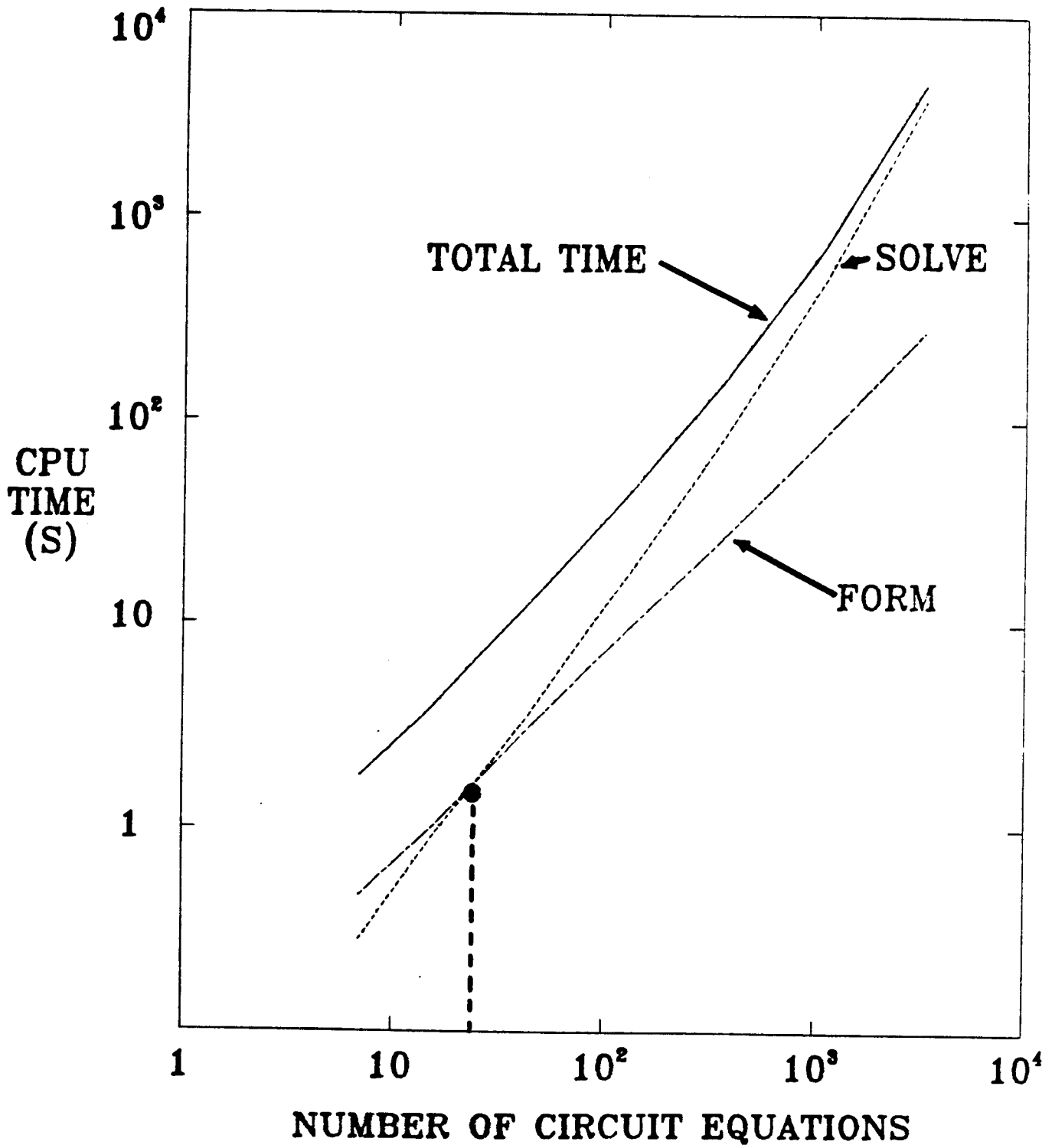
using a damped Newton-Raphson linearization process.  $G$  is the Jacobian matrix (or the small-signal conductance matrix),  $V$  is the unknown voltage vector and  $I$  is the known excitation vector. Finally, (2-2) is solved using a direct matrix approach to produce the solution vector,  $V$ .

### 2.3. Motivation for a New Simulation Approach

General-purpose simulation programs such as SPICE2 [6] and ASTAP[13] have been used extensively to perform accurate circuit analysis for over 10 years. These simulators use direct methods (using sparse matrix techniques) to solve the set of circuit equations. Unfortunately, the cost of using these simulators in terms of computer CPU-time and memory requirements becomes prohibitive as the size of the circuit increases. The fundamental problem is illustrated in Fig. 2.1. While the time required to formulate the equations grows linearly with circuit size, the solution time is proportional to  $N^k$  where  $N$  is the number of circuit nodes and  $k$  ranges from 1.1 to 1.5. This is one reason why the direct approach becomes increasingly expensive as the circuit size increases.

Timing simulation was introduced in the mid-seventies to reduce CPU-time at the expense of some accuracy. A new breed of simulators emerged at that time, all tailored to handle the transient analysis of large digital cir-

Figure 2.1 : Equation Formulation and Solution times  
for standard circuit simulation



cuits[5, 4, 1, 14, 15] . These classical timing analysis programs used iterative techniques [16] to solve the set of circuit equations rather than the direct matrix solution approach of the previous generation. A grounded capacitor was required at every node to guarantee convergence of the method. However, to reduce the execution time, none of these programs carried the iteration to convergence and in fact each node equation was only solved once at each timepoint.

Large digital circuits typically displays a 10-20 % *latency* characteristic. That is, only 10-20 % of the nodes in the circuit are active at any given time. Conceptually, there is temporal sparsity (latency in a waveform over a time period) and spatial sparsity (latency in the network at a given point in time[17] . Since these iteration methods involve the solution of each equation separately, this latency aspect could be exploited to further improve performance.

Using these techniques, two orders of magnitude of speed improvement was obtained. Accuracy was maintained in these simulators by choosing a small fixed timestep for the entire analysis. This timestep was either constant for all circuits [5] or chosen based on the smallest time constant in the circuit[4] . Later timing simulators adjusted the timestep during the analysis dynamically to limit the voltage change over a timestep to a value specified by the user[1] . Simple timing analysis also relied heavily on the fact that the accumulated error becomes zero once a node reaches either of the two supply voltages.

While offering a substantial savings in CPU-time and memory usage, these programs suffer from a number of problems which has limited their use. Circuits containing global feedback loops, such as the ring oscillator of

Fig 2.2(a), introduce timing and voltage errors into the simulation. Fig 2.2(b) illustrates these errors as generated by SPLICE1.3 compared to the solution produced by SPICE2. The SPLICE1.3 program not only produces a timing error (phase error) but incorrectly predicts the number of cycles in a given time period (frequency error) and the height of the peaks (amplitude error).

These errors are all due to the single iteration performed at each timepoint. To understand the origin of the errors, consider the example of a simple NMOS inverter of Fig. 2.3(a) and examine the processing sequence in NTA:

- (1) The first step is to convert each non-linear device to its corresponding companion model. This is done in Fig. 2.3(b). These equivalent models are based on the terminal voltages of each device. The conductance is obtained from the slope of the non-linear I-V characteristic at the operating point and the current is obtained from the y-axis intercept as shown in Fig. 2.3(c). The value of the voltage at Node  $C$  is calculated using this equivalent circuit of Fig. 2.3(b). Assume that initially  $V_B^{n-1}=0v$  and  $V_C^{n-1}=5.0v$ , where  $V_B^{n-1}$  means the voltage at node  $B$  at time  $t_{n-1}$  and  $V_C^{n-1}$  has a similar definition.
- (2) Let  $V_B^n=1.0v$ . Then the change in the voltage at node  $C$  is calculated using  $V_B^n$  and  $V_C^{n-1}$ . Therefore, the linear equivalent model is the same as it was at  $t_{n-1}$  but the equivalent model of the driver changes. Since load offers less charging current than it really should (i.e.,  $V_C$  is incorrect) and the driver is able to sink more current due to a larger  $V_{ds}$ , the node voltage change  $\Delta V_C^n$  is too optimistic.
- (3) When  $V_B^{n+1}=2.0v$ , again  $V_C^{n+1}=f(V_C^n, V_B^{n+1})$  and  $\Delta V_C^{n+1}$  is also optimistic by the same argument given above.

Figure 2.2(a) : NMOS Ring Oscillator Circuit

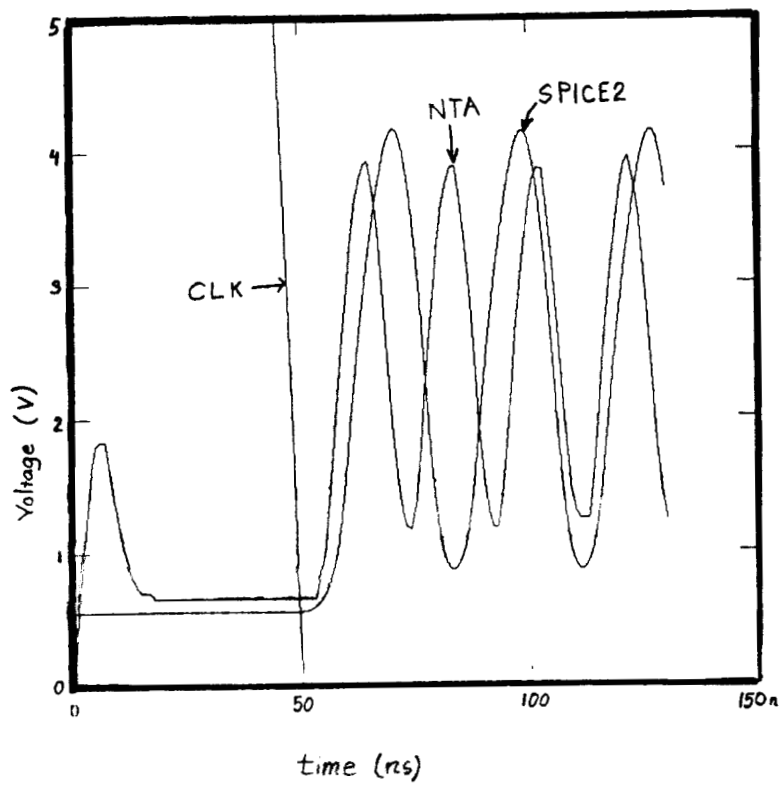
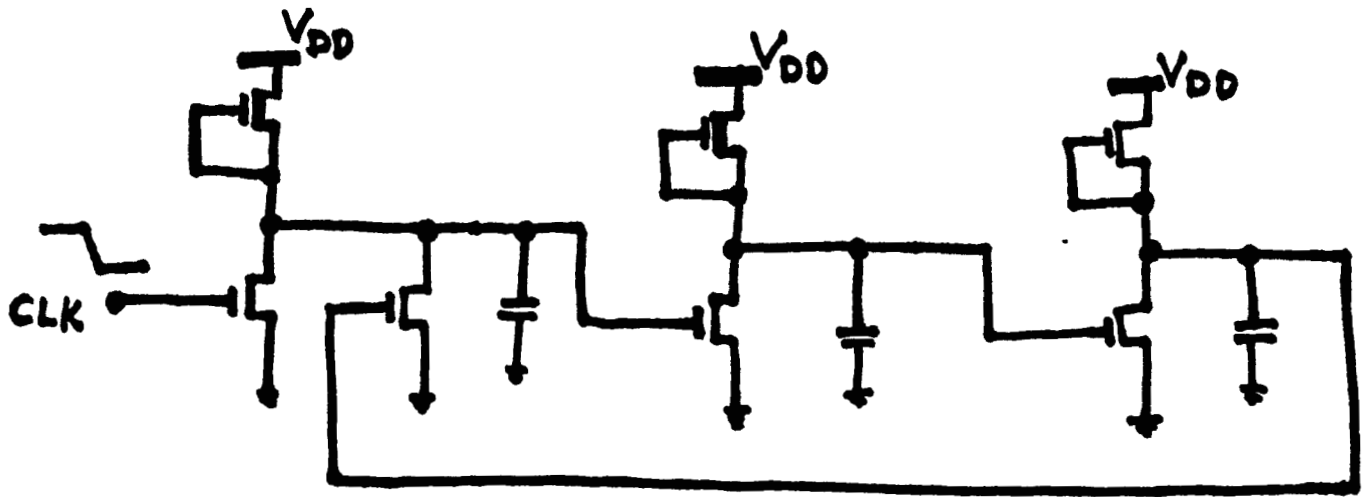
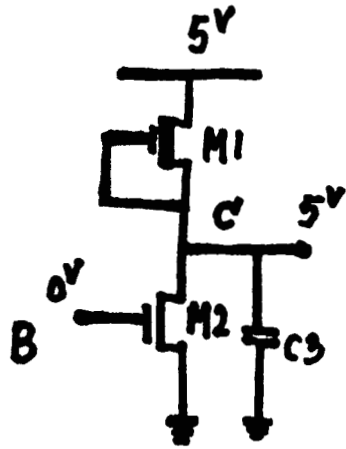
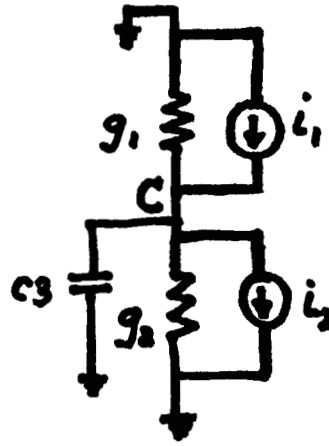


Figure 2.2(b) SPICE2/SPLICE1.3 Comparison

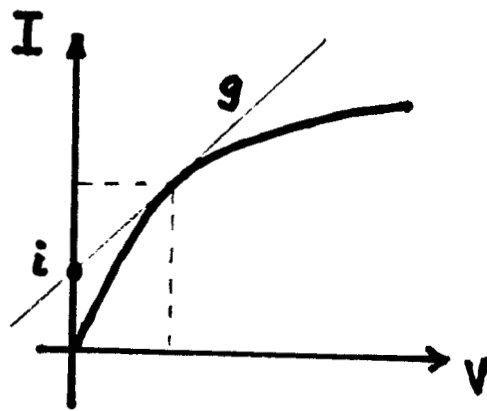
Figure 2.3 : Linear equivalent models



(a)



(b)



(c)

Hence, in a SPLICE1.3 simulation, the output of the inverter will rise and fall much earlier and faster than the SPICE2 simulation of the same circuit. This error is propagated and intensified in the ring oscillator circuit, resulting in all three errors cited above. It should be noted that if the timestep of the simulation is reduced and the accuracy tolerances are tight, the NTA output will be indistinguishable from SPICE2 output for this example.

Another shortcoming of NTA is that it has some difficulty dealing with circuits containing floating elements, such as capacitors and transfer gates. These elements introduce strong bilateral coupling between two nodes in the circuit. Since only one iteration is used, the solution obtained using NTA is inconsistent. That is, the final node voltage values depend on the order that the nodes are processed. Consider, for example, the 2-input NMOS nand circuit of Fig. 2.3(d). It contains a "floating" transistor, namely M2. The sequence of processing in the NTA method would be as follows :

- (1) Assume that initially  $V_X^{n-1}=0v$ ,  $V_Y^{n-1}=5.0v$  and  $V_W^{n-1}=0v$
- (2) At  $t_n$ ,  $V_W^n=1.0v$  and Node X is processed using the initial conditions  $V_X^{n-1}$  and  $V_W^{n-1}$  given above to produce  $V_X^n$ .
- (3) Next, Node Y is processed using  $V_Y^{n-1}$  and  $V_X^n$  to generate  $V_Y^n$ .
- (4) Then, time is advanced by one unit and steps (2) to (4) are repeated. This process continues until Node Y makes its transition to the opposite rail voltage.

There are two problems with this method:

- the change in node Y should immediately affect node X but it is not reflected at node X until the next time point.

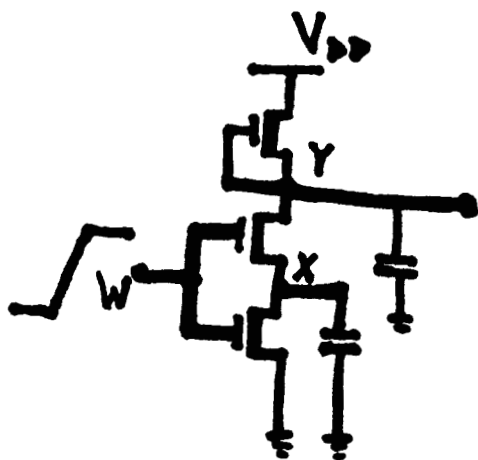


Figure 2.3 (d) : 2-input NMOS NAND circuit

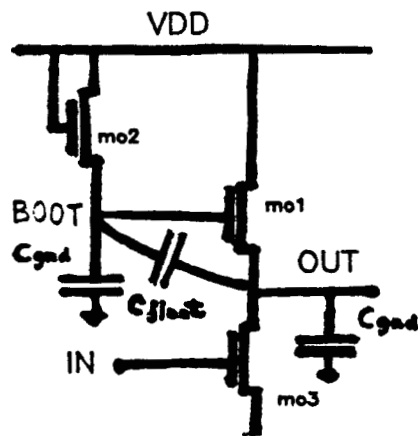


Figure 2.4 : Boot-strapped Inverter

- if the processing started with node Y instead of node X, slightly different results would be obtained.

The same effect is observed when processing capacitors where one node is not connected to ground (i.e., a floating capacitor). An example of a circuit with such a capacitor is the boot-strapped inverter of Fig 2.4. The accuracy of NTA depends on the timestep and the ratio of the floating capacitor to the grounded capacitor. In the boot-strapped inverter, the value of  $C_{float}$  is usually large compared to the grounded capacitors and this tends to reduce the accuracy of the solution produced by NTA.

Therefore, it is clear that NTA will produce inaccurate results when there are floating elements in the circuit. Reducing the timestep to an appropriate value will improve the accuracy. If the timestep is not small enough, these elements may cause the simulator to exhibit instability. As will be seen later in this section, the ITA approach overcomes all of these problems.

By far the most compromising aspect of the NTA approach is that it may occasionally produce the wrong answer! Circuit designers are willing to use a program which gives them the correct answer or no answer (usually due to non-convergence), but are unable to deal with a program that occasionally produces the wrong answer. In fact, the NTA method *always* produce some answer and this is really the downfall of the method.

For all of the reasons given above, timing analysis has not been widely accepted as viable form of electrical simulation, although it has been used successfully in constrained IC design methodologies such as standard cell or gate array. What is really required is a simulation technique which provides both accuracy and speed.

## 2.4. Relaxation-based Electrical Simulation

A number of new techniques have been developed in an effort to reduce the simulation time while maintaining waveform accuracy comparable to SPICE2. These include table-driven model evaluation [11], microcode tailoring on a minicomputer [18] and the use of vector-oriented computers such as the CRAY-1[19]. Although these techniques have been successful, they provide, at most, an order of magnitude speed improvement over SPICE2.

Two methods are currently being investigated which use a converged relaxation iteration to solve the set of circuit equations. Both approaches have been implemented and preliminary results indicate that up to two orders of magnitude of speed improvement may be obtained for large digital circuits. One method, called *Waveform Relaxation*[20], decomposes the system of equations into several dynamic subsystems each of which is analyzed for the entire simulation period. The process is then repeated until all the waveforms converge to an exact solution. The relaxation is performed at the differential equation level. This method has been implemented in program RELAX.[20,21]

The second method, called *Iterated Timing Analysis* (ITA) [22,23]. In this method, the relaxation is performed at the non-linear equation level. That is, the set of *non-linear* circuit equations are iterated to convergence using a Gauss-Seidel or Gauss-Jacobi method. This is also an exact method. Some aspects of this method which make it attractive are as follows:

- it has guaranteed convergence and stability properties
- it allows circuit latency to be exploited easily
- it can be implemented using the concepts developed for logic simulation

- since the logic and electrical analysis operate the same way, a consistent mixed-mode simulation is possible

The algorithm has been implemented in SPLICE1.6 and the implementation details and results obtained are presented in this chapter following a simple mathematical treatment of the method.

## 2.5. The ITA Algorithm

### 2.5.1. The Gauss-Seidel Iteration Method

A system of simultaneous *linear* equations can be solved using a variety of techniques, namely:

1. Direct Methods
  - a. Matrix Inversion
  - b. Gaussian Elimination
  - c. LU decomposition
2. Iterative Methods
  - a. Gauss-Jacobi
  - b. Gauss-Siedel
  - c. SOR-Newton
  - d. Newton-SOR

In circuit simulation, the solution to Eqn. (2-2) is required. The circuit conductance matrix,  $G$ , is usually large but sparse, typically having 3 elements per row. Matrix inversion is not a suitable method because it usually converts a sparse matrix into a dense one. Sparse matrix techniques can be used to solve the equations using method 1(a) or 1(b) but this is a time-consuming task, as evidenced by Fig. 2.1.

The iterative methods [16] are well-suited to cases where the matrix is sparse and, in fact, a solution may be obtained faster than a direct method in some cases. Two classical iteration methods exist: the Gauss-Jacobi (G-J)

method and the Gauss-Seidel (G-S) method. The Gauss-Jacobi method (also referred to in the literature as simultaneous displacement) proposes the following approach:

$$\begin{aligned}
 &v^{(0)} = \text{initial guess voltage vector} \\
 &m \leftarrow 0 \\
 &\text{repeat } \{ \\
 &\quad \text{for } (i = 1 \text{ to } N) \{ \\
 &\qquad v_i^{m+1} = \frac{1}{g_{ii}} \left[ i_i - \sum_{\substack{j=1 \\ j \neq i}}^n g_{ij} v_j^m \right] \\
 &\quad \} \\
 &\quad m \leftarrow m + 1 \\
 &\} \text{ until } |v_i^{m+1} - v_i^m| \leq \varepsilon \text{ for all } i, \text{ i.e., convergence}
 \end{aligned} \tag{2-3}$$

Notice that every equation uses the *previous* iteration values for all unknown voltages to obtain a new solution vector. The Gauss-Seidel method (also referred to as successive displacement) suggests the following modification to Gauss-Jacobi:

$$\begin{aligned}
 &v^{(0)} = \text{initial guess voltage vector} \\
 &m \leftarrow 0 \\
 &\text{repeat } \{ \\
 &\quad \text{for } (i = 1 \text{ to } N) \{ \\
 &\qquad v_i^{m+1} = \frac{1}{g_{ii}} \left[ i_i - \sum_{j=1}^{i-1} g_{ij} v_j^{m+1} - \sum_{j=i+1}^n g_{ij} v_j^m \right] \\
 &\quad \} \\
 &\quad m \leftarrow m + 1 \\
 &\} \text{ until } |v_i^{m+1} - v_i^m| \leq \varepsilon \text{ for all } i, \text{ i.e., convergence}
 \end{aligned} \tag{2-4}$$

Notice that each equation uses the *latest* values of voltage wherever possible.

The only difference in the two methods is whether the previous voltages are always used or the latest values are applied immediately. The convergence rate is linear in both cases but the speed of convergence is quite different. In general, the Gauss-Seidel iteration converges faster than

Gauss-Jacobi [16] although examples can be constructed where this is not true.

Both methods also require the strict diagonal dominance condition for guaranteed convergence:

$$\sum_{\substack{j=1 \\ j \neq i}}^n |g_{ij}| < |g_{ii}| \quad (2-5)$$

This inequality states that each diagonal term of the matrix be greater than the sum of all the off-diagonal terms in the same row.

An acceleration scheme is available to speed up convergence by introducing an acceleration parameter,  $\omega$ , as follows.

$$v_i^{m+1} = \omega v_i + (1-\omega)v_i^m \quad (2-6)$$

where  $v_i$  is an intermediate value generated using Eqn. (2-4). The effect of  $\omega$  is usually dramatic but it can only be obtained empirically and usually varies from technology to technology. For standard Gauss-Seidel,  $\omega = 1$ .

### 2.5.2. A Non-Linear Gauss-Seidel Iterative Approach

Relaxation methods, as described in the previous section, can also be applied successfully at the non-linear equation level. The total number of iterations may be reduced by using a property of the non-linear iteration. The reason for this will be made clear in Sec. 2.5.4.

The following is a description of how this is done is SPLICE1.6. Starting with equation (2-1), the first step is to convert the differential equations into difference equations using a stiffly-stable integration formula. SPLICE1.6 uses a Backward-Euler formulation[24]. Then the first equation is linearized using the Newton-Raphson (N-R) method and iterated to convergence to solve

for one unknown voltage. This constitutes the inner N-R loop. The same process is applied to the next equation and all subsequent equations, in turn, until the last equation is processed. This outer G-S loop is now iterated to convergence to produce the solution.

To further illustrate the method, consider the solution method applied to one node in a typical circuit. Fig 2.5(a) shows three non-linear devices connected to Node 4 which itself has a capacitor connected to ground. We begin by writing KCL for Node 4

$$\sum_{j=1}^4 I_j = I_4 - I_1 - I_2 - I_3 = 0 \quad (2-7)$$

This can be rewritten in the form of Eqn. (2-1) :

$$C_4 \dot{V}_4 = I_1(V_1, V_4) + I_2(V_2, V_4) + I_3(V_3, V_4) \quad (2-8)$$

Using the Backward-Euler formula for  $I_4$ , we obtain

$$I_4 = C_4 \frac{dV_4}{dt} = \frac{C_4}{h} (V_{4(n)} - V_{4(n-1)}^*) \quad (2-9)$$

where  $h$  is the integration step size,  $V_{4(n)}$  means the voltage value for Node 4 at time  $t_n$  and  $V_{4(n-1)}^*$  refers to the solution obtained for Node 4 at time  $t_{n-1}$ . Therefore, Eqn. (2-8) can now be written as a difference equation,

$$\frac{C_4}{h} (V_{4(n)} - V_{4(n-1)}^*) - I_1(V_1, V_4) - I_2(V_2, V_4) - I_3(V_3, V_4) = 0 \quad (2-10)$$

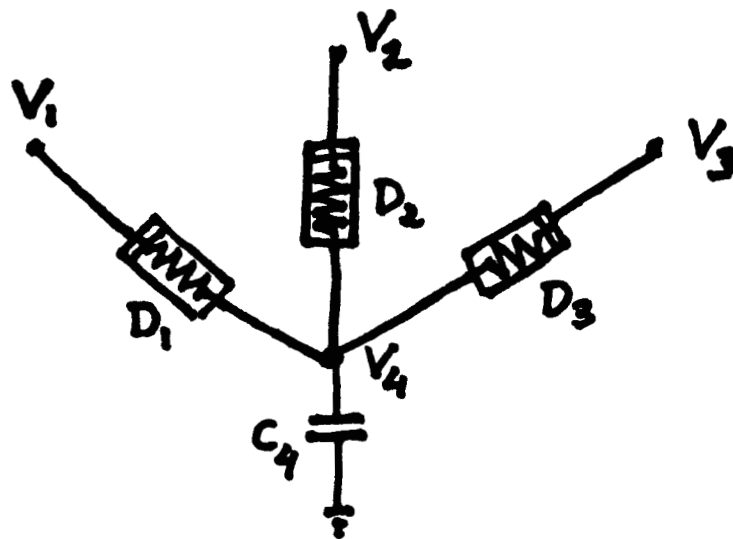
Since Eqn. (2-10) has the form:

$$f(V_1, V_2, V_3, V_4) = 0 \quad (2-11)$$

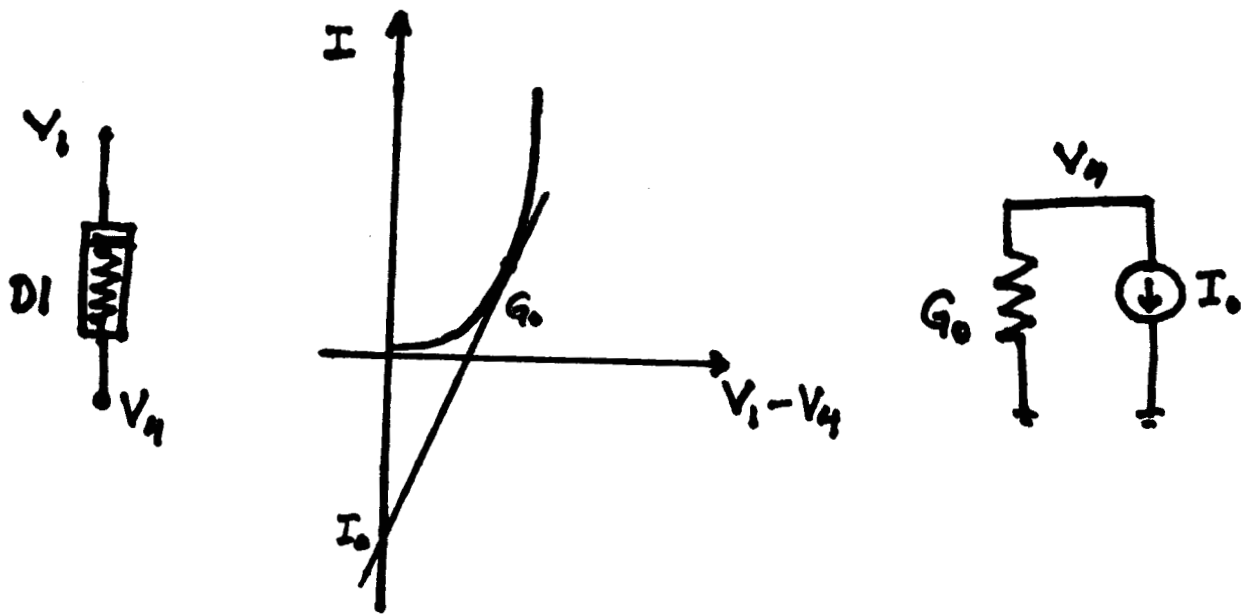
it is suitable for the Newton-Raphson (N-R) iterative method with  $V_4$  as the unknown variable. The general equation for one N-R iteration is

$$x^{(i+1)} = x^{(i)} - \frac{f(x^{(i)})}{f'(x^{(i)})} \quad (2-12)$$

Figure 2.5 : Non-linear Gauss-Seidel Calculations



(a)



(b)

In circuit terms, the N-R calculation usually requires that a linear equivalent be determined for each non-linear device connected to the node, as shown in Fig. 2.5(b) for D1. This involves the calculation of a conductance,  $G_0$  and a current intercept,  $I_0$ . In order to avoid the intercept calculation, we can apply Eqn. (2-11) directly to Eqn. (2-12) to get

$$V_{4(n)}^{i+1} = V_{4(n)}^i - \frac{f(V_1, V_2, V_3, V_4)}{f'(V_1, V_2, V_3, V_4)} \quad (2-13)$$

Now set  $\Delta V_{4(n)}^{i+1} = V_{4(n)}^{i+1} - V_{4(n)}^i$  and substitute Eqn. (2-10) into Eqn. (2-13) to get

$$\Delta V_{4(n)}^{i+1} = \frac{\sum_{j=1}^3 I_j^i - \frac{C_4}{h}(V_{4(n)}^i - V_{4(n-1)}^*)}{\sum_{j=1}^3 G_j^i + \frac{C_4}{h}} \quad (2-14)$$

where  $V_{4(n)}^i$  refers to the  $i$ th iteration value of voltage at Node 4 at time  $t_n$  and  $I_j^i$  refers to the  $i$ th iteration value of current at Node  $j$ . This method of evaluating  $\Delta V$  is convenient because:

- no intercepts need to be calculated since total currents are used in Eqn. (2-14)
- current levels are within operating ranges (unlike  $I_0$  in Fig. 2.5(b))
- the value of  $\Delta V$  is very accurate when calculated this way. Note that  $\Delta V$  is the difference between two Newton iterations and it will tend toward zero with each iteration. Therefore it should be calculated as accurately as possible.

For an arbitrary node Eqn. (2-14) becomes

$$\Delta V^{i+1} = \frac{\sum_j^n F_j^i - \frac{C}{h}(V_n^i - V_{(n-1)}^i)}{\sum_j^n G_j^i + \frac{C}{h}} \quad (2-15)$$

### 2.5.3. The SOR-Newton Iteration

A combination of the Newton-Raphson iteration in a converged Gauss-Seidel loop with acceleration applied is called an SOR-Newton Iteration. In equation form, it is simply

$$\Delta V = -\frac{\omega f(V)}{f'(V)} \quad (2-15)$$

In a standard N-R iteration, the equation is iterated until  $|\Delta V| \leq \epsilon$ . This means that each node equation should be iterated to convergence before moving on to the next one. The Gauss-Seidel loop (i.e., the outer loop) must also be iterated to convergence.

### 2.5.4. Convergence of the SOR-Newton Iteration

A very important property of the SOR-Newton iteration can be applied now to greatly reduce the number of iterations of the inner N-R loop. It happens that *one* Newton iteration per equation for each G-S iteration is sufficient to retain the convergence properties of the non-linear Gauss-Seidel iteration[16] as long as the convergence requirements of the N-R iteration are strictly satisfied.

A Newton-Raphson iteration will converge if the initial guess is "close enough" to the **exact** solution, given that the function is Lipschitz continuous. Under these conditions, the rate of convergence is quadratic. Since the element model equations are smooth, the solution from one timepoint to the next will not be drastically different. Therefore, the solution at the previous

timepoint is a good first guess for the N-R iteration. Convergence may be enhanced by using a prediction step based on the last few solution points. A simple linear predictor is used in SPLICE using the previous two solution points.

The diagonal dominance condition of the G-S iteration must also be satisfied to guarantee the convergence of the SOR-Newton iteration. In circuit terms, this requirement can always be met by putting a grounded capacitor at every node and choosing an appropriate timestep. Grounded capacitors appear as  $\frac{C}{h}$  terms in the diagonal position of the conductance matrix  $G$ . Therefore,  $h$ , which is the simulation timestep, can be reduced until the  $\frac{C}{h}$  term outweighs all off-diagonal terms. Obviously, the capacitance value,  $C$ , can be increased to achieve the same effect but usually the capacitance is determined from the IC layout and therefore cannot be adjusted.

Off-diagonal terms appear in the conductance matrix when there is coupling between two nodes. For example, when floating capacitors are used,  $\frac{C}{h}$  terms appear in diagonal and off-diagonal positions. Therefore, increasing the value of  $C$  or reducing the value of  $h$  is not as effective and this may lead to convergence problems. The ratio of the floating capacitor to the grounded capacitor is an important factor in determining the speed at which convergence is achieved. If the floating capacitor is very large compared to the grounded capacitor, convergence speed will be slow, if the iteration converges at all. The current version of SPLICE uses the IIE method (Implicit-Explicit) [25] to handle floating capacitors.

## 2.6. Implementation in SPLICE

The analysis techniques described in the previous sections have been implemented in SPLICE1.6. The details are described in this section with special attention given to areas where further optimization would improve the simulator performance.

SPLICE1 has a fixed simulation timestep called the **mrt** (minimum resolvable time). Events can only be scheduled at integer multiples of **mrt**. There is a scheduling threshold parameter called **mindvsch** which is the minimum change in a node voltage over a timestep which causes the fanout elements of the node to be scheduled. The convergence criteria is defined by two parameters called **abstol** (absolute tolerance) and **reltol** (relative tolerance).

### 2.6.1. Program Flow

The program flow has not changed since the SPLICE1.3 release. The details of the processing may be found in [1, 3] and are not repeated here. The data structures of the ITA as implemented in SPLICE1.6 are given in APPENDIX II. The general program flow for electrical analysis is as follows:

```

set all nodes to their initial values ;
schedule all FOL's at time 0 ; #FOL = FanOut List of a node
 $t_n = 0$  ;
while (  $t_n < TSTOP$  ) {
  foreach (FOL in the queue at the current timepoint) {
    foreach (element in the FOL) {
      foreach (output node of an element) {
        process node ; #see next section for details
        schedule FOL if necessary ;
      }
    }
  }
  plot all requested active nodes ;
   $t_n = t_n + 1$  ;
}

```

}

### 2.6.2. Details of Node Processing

A subroutine in SPLICE1.6 processes all electrical nodes, calculates the new node voltage, decides whether the node has converged and determines whether subsequent scheduling is necessary. A high-level pseudo-code description of the routine is as follows:

```

begin
# Iterated timing analysis algorithm in SPLICE1.6
# Node processing sequence
  pick up next node i;
  if (first time processed at new timepoint) {
    use last two points to perform linear prediction ;
    convflg=false ;
  }
  Gnet = Inet = 0 ;
  for ( each fanin element at node i ) {
    compute equivalent conductance Geq;
    compute total current flowing into node Ieq;
    Gnet = Gnet + Geq;
    Inet = Inet + Ieq;
  }
  calculate  $\Delta V$  ; #change in voltage over an iteration
   $V_n^{(i+1)} = V_n^{(i)} + \Delta V$  ; #new node voltage
   $DV = |V_n^{(i+1)} - V_{n-1}|$  ; # change in node voltage over one timestep
  if ( $\Delta V < \text{tolerance}$ ) { # node has converged
    if (convflg = false) { #have not converged at this timepoint before
      if (  $DV > \text{mindvsched}$  ) { # node change is significant
        schedule current fol at  $T_{n+1}$  (future);
        schedule fol of node at  $T_n$  (now) ;
        convflg = true ;
      }
      else { # node change is not significant over one timestep
         $V_n = V_{n+1}$  ; #restore old value
      }
    }
    else #have converged previously at this timepoint
      do nothing ; #break any feedback loops
  }
  else { # node has not converged so keep processing
    convflg = false ;
    schedule current fol at  $T_n$  (now) ;
    schedule fol of node at  $T_n$  (now) ;
  }
}

```

```
# Finished this node for this iteration  
return  
end
```

### 2.6.3. Element Models

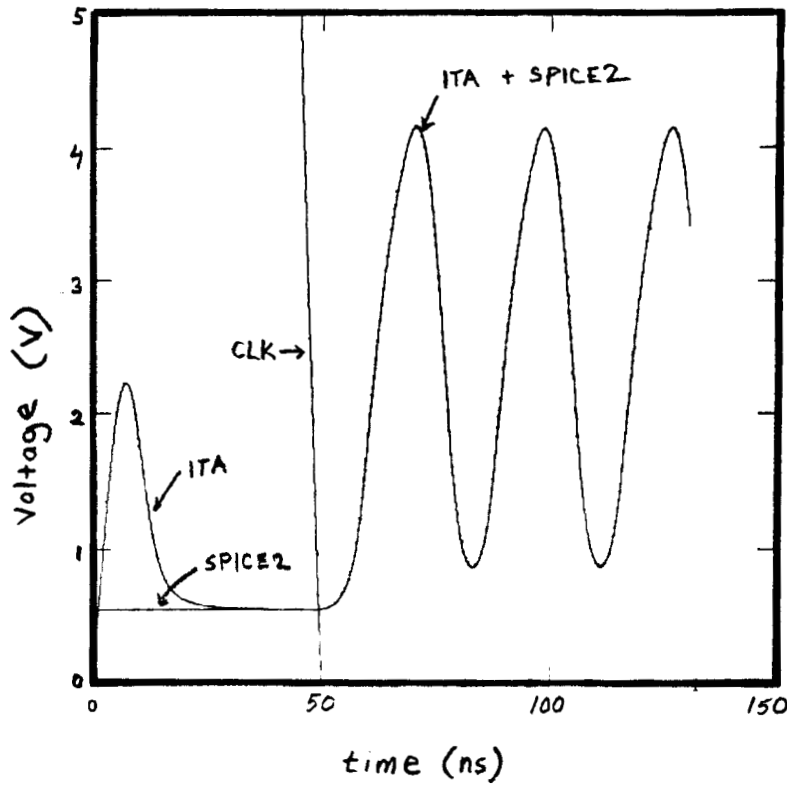
SPLICE1.6 has built-in models for resistors, linear capacitors (floating and grounded), and MOS transistors. The IIE method is used to handle floating capacitors [25] and the first-order Schichman-Hodges model [26] equations are used to handle the MOS transistors. The model equations used for each of the devices are given in APPENDIX III.

Each electrical element has a corresponding program subroutine. The subroutine evaluates the linear equivalent model for each non-linear device and returns it to the calling routine. As mentioned previously, the intercept current calculation can be avoided by a simple reformulation of the equations. Using this approach, the conductance and the *total* current at a given operating point is returned by each subroutine. The calculation of the equivalent model assumes that all other nodes have ideal *constant* voltage sources attached to them.

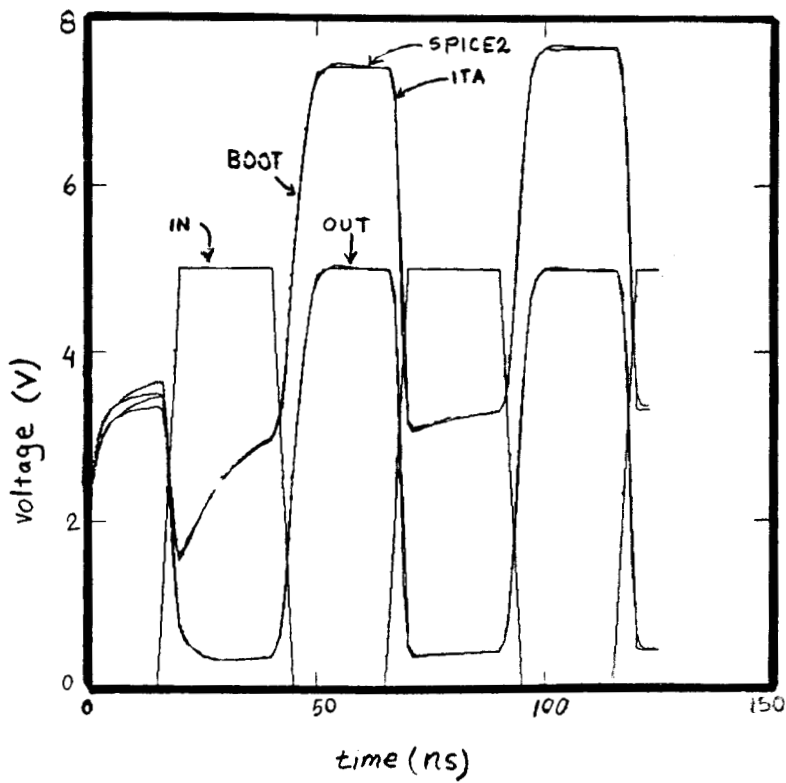
## 2.7. ITA Simulation Results

This chapter has been concerned mainly with simulation accuracy and it would not be complete without a comparison of ITA with SPICE2. Fig. 2.6 shows the simulation results obtained for the ring oscillator, 2-input NAND and boot-strapped inverter circuits described earlier. As indicated by the results, SPLICE1.6 produces results which are indistinguishable from those obtained by SPICE2 except at timepoints near time zero due to different initial value assumptions. It will be shown later in Chap. 4 that the ITA method

Figure 2.6 : Accuracy Comparison of SPICE2 and ITA

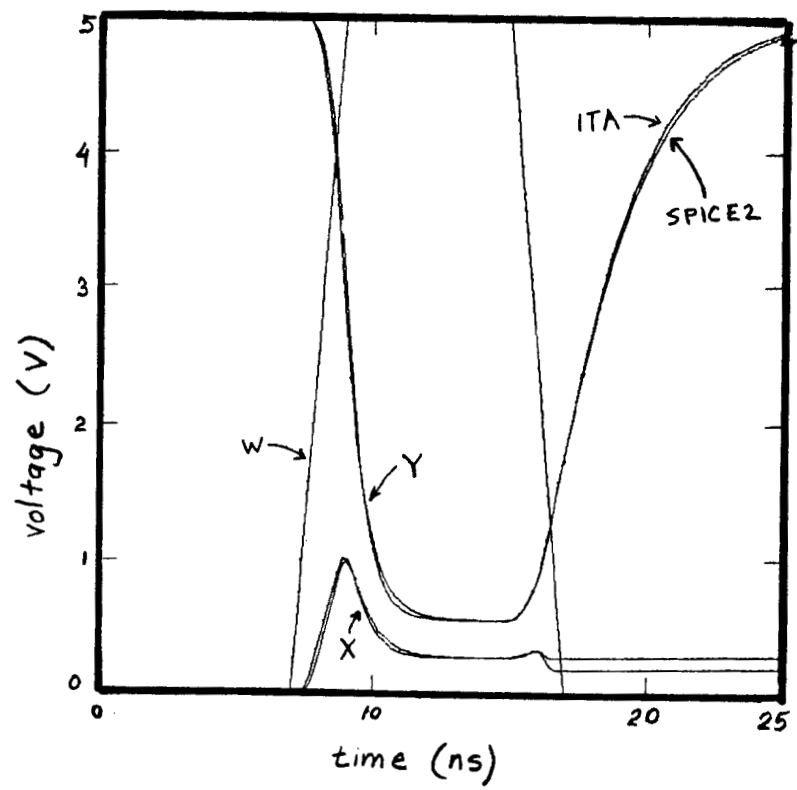


(a) Ring Oscillator of Fig. 2.2(a)



(b) Boot-strapped Inverter of Fig. 2.4

Figure 2.6 (c) : NAND circuit of Fig. 2.3(d)



is robust enough to handle complex analog circuits such operational amplifiers in a unity-gain configuration. Therefore, circuits which handled inadequately using NTA do not pose a problem to ITA in terms of accuracy.

The run-times of the 3 examples do not demonstrate the speed advantage of ITA because the circuits are all very small with dense G matrices and the activity is high. The selective trace feature in SPLICE can only be used to advantage in very large circuits.

## 2.8. Optimizations in the Present Implementation

While the data structures used in SPLICE1 are well-suited to handle circuit, timing and logic simulation concurrently, they are not ideal for ITA. If a separate program were written to perform ITA, several optimizations could be made to improve the program performance.

For instance, some nodes are accidentally reprocessed after they have converged because there may be several paths to the same node through different elements. Therefore, a node may be processed twice in succession before another node is processed (i.e., two Newton iterations). Also, there is a lot of time spent "walking" through the fanout lists and element tables to reach a node, as shown in a previous section.

These problems can be eliminated by scheduling and processing *nodes* as opposed to fanout lists. A double buffer scheme at each timepoint could be used to avoid the accidental reprocessing of a node before all other active nodes are processed, as follows:

```

put all nodes in event list  $E_A(0)$ ;
 $t_n = 0$ ;
while (  $t_n < TSTOP$  ) {
     $k \leftarrow 0$ ;
    while ( event list  $E_A(t_n)$  is not empty ) {
        foreach (  $i$  in  $E_A(t_n)$  {

```

```

    obtain  $\Delta V$ ;
     $v_i^{k+1} = v_i^k + \Delta V$ ;
    if (  $|v_i^{k+1} - v_i^k| \leq \epsilon$  ) { i.e., if convergence is achieved
        add node  $i$  to list  $E_A(t_{n+1})$ ;
    }
    else {
        add node  $i$  to event list  $E_A(t_n)$ ;
        add fanout nodes of node  $i$  to event list  $E_A(t_n)$ 
        if they are not already there;
    }
}
 $E_A(t_n) \leftarrow E_B(t_n)$ ;
 $E_B(t_n) \leftarrow \text{empty}$ ;
}
 $t_n \leftarrow t_{n+1}$ ;  $t_{n+1} = \text{next timepoint}$ 
}

```

Another problem in the current program is that if it does not converge at a timepoint, the program simply stops execution. The user must decrease the timestep manually and re-run the entire simulation. An automatic internal timestep control mechanism would be useful not only for the convergence problem but also for error control. If the error is small at a particular timepoint, then the timestep could be increased. If the error is too large, the timestep could be decreased. The nodes would then be re-evaluated at the new timepoint. Hence, the timestep could be computed based on an estimate of the Local Truncation Error. Each node could have its own mrt, independent of other nodes, as long as some consistency is maintained in the simulation between different nodes. Unfortunately, dynamic timestep control requires the ability to "backup" in time (i.e., a buffering of previous results for each node) and requires a modification of the data structures to allow successive refinement of the mrt (minimum resolvable time) in the time queue [27]. For this reason, it would require a lot of effort to implement this scheme in the current SPLICE1 environment.

## CHAPTER 3

### 3. Enhancements to the Logic Analysis

#### 3.1. Introduction

The improvements made to the logic analysis in SPLICE1 are described in this chapter. The starting point of this work was SPLICE1.3. It had the following features:

- a 4-state logic model (0,1,X,Z)
- fixed assignable rise and fall delays on all gates
- unidirectional and some bidirectional elements handled.

There have been a number of changes in the logic analysis since the SPLICE1.3 release. These changes were made to alleviate some of the problems in the previous version and to facilitate conversions in the mixed-mode environment.

The new version is SPLICE1.6 which features:

- a new MOS-oriented state model
- a fanout dependent delay model
- unidirectional and generalized bidirectional element processing.

The logic analysis is performed using a relaxation-based method, similar in nature to the electrical analysis. In fact, the logic analysis can be thought of as an implementation of non-iterated timing analysis (see Chap. 2) with simplified element models. Each logic node carries information about the node voltage and the equivalent conductance-to-ground, as does the electrical node. Therefore, the mixed-mode interface is defined in a consistent manner in SPLICE1.6.

This chapter begins with a description and definition of the new state model. Following this, the delay model is described. Then, the "spike" detection and handling procedure is presented. A spike is a pulse at a node of shorter duration than the minimum width necessary to trigger subsequent gates. This is usually an error condition which must be identified and reported to the user.

In the next section, the important issues surrounding the MOS transfer gate are reviewed. The transfer gate (or transmission gate, or pass transistor) is the source of all MOS modeling problems at the logic level and the reason for this will become clear in this chapter. Next, the logic analysis algorithm will be presented in detail. SPLICE1.6 can also be used to perform switch-level simulation [9, 10] and this is described in the last section. Background material on MOS logic simulation may be found in reference[3].

## **3.2. The State Model**

### **3.2.1. A MOS-oriented Logic Model**

Most modern logic simulators handle the problems specific to MOS integrated circuits by including the notion of *signal strength*[7, 8, 9, 10] in the logic model. The rationale for this has been presented in a previous publication[3]. Strength is an abstraction of the large-signal conductance from a node to ground or from a node to a supply voltage. It can be associated with the output of a gate or it can be an attribute of a node. For instance, in the inverter of Fig. 3.1 (M1 and M2), the driver transistor with its gate input at 5.0V represents a very low resistance path from Node B to ground. In MOS logic model terms, this is referred to as a "forcing 0" or "driving 0". Simi-

Figure 3.1 : Logic Strength Definitions

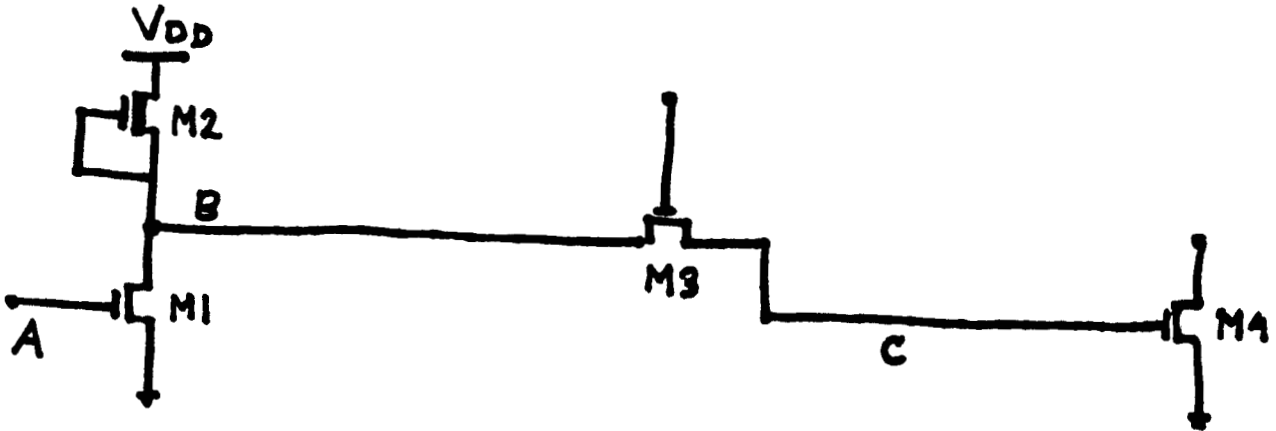
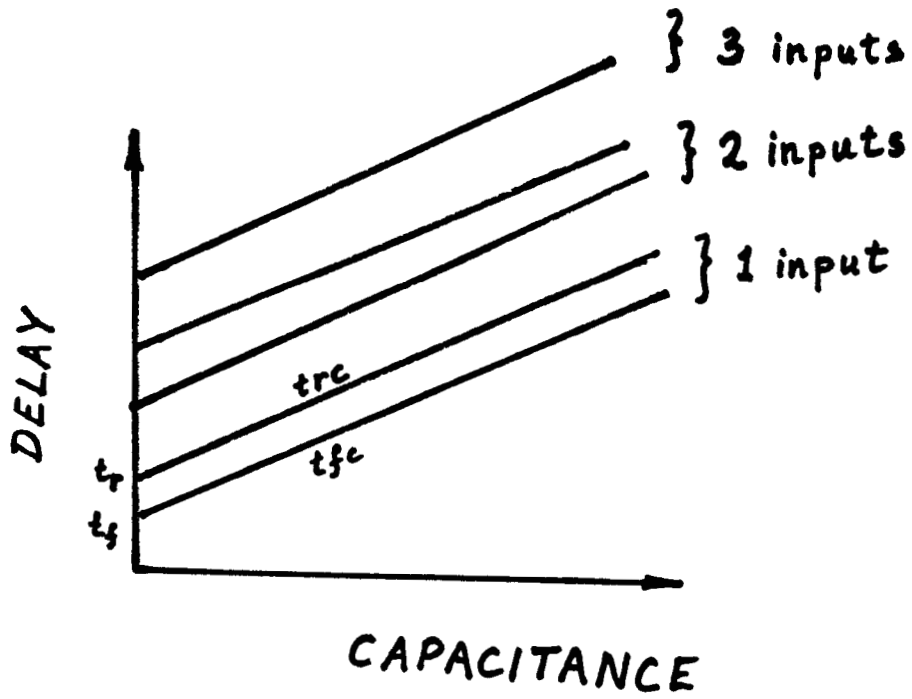


Figure 3.2 : Delay Modeling for Basic Gates



larly, the load transistor represents a sizeable resistance from Node B to VDD (approx. 20k $\Omega$  to 40k $\Omega$ ) and this is referred to alternatively as a "soft 1", a "resistive 1" or a "weak 1". If transistor M3 is turned "OFF" (that is, if the gate voltage is zero for an NMOS transistor), Node C goes into a "high-impedance" condition which represents a third distinct strength. Although most simulators are based on these three strengths, SPLICE1.6 allows up to  $2^{16} - 1$  strengths for two reasons:

- there is a requirement for more than three strengths when modeling the interaction of several transfer gates with differing W/L ratios, typically found in bus contention situations.
- it provides a mechanism for consistent signal representation in the logic domain for schematic or mixed-mode simulation[22] . If information about the effective conductance to ground is stored with each electrical node, this information could be converted to a strength value and passed on to the logic node, along with the voltage information, whenever there is a requirement to do so. Conversions in the opposite direction can be performed in a similar manner. In this way, simulation accuracy can be maintained in the mixed-mode environment.

### 3.2.2. State Model Definition

The state model used in SPLICE1.6 is now formally defined :

- A state is composed of a logic level, logic strength pair (L,S).  
i.e.,state=(L,S)=(Level,Strength)
- The logic level can be one of three values: logic zero(0), logic one(1) or logic unknown(X). The "0" level represents the low threshold value or ground. The "1" level represents the high threshold value or VDD. The

"X" level represents an undetermined value which could be "0", "1" or some value in between. The logic level field is extracted from the state using the "lev" function. That is,

$$L = \text{lev}(\text{state})$$

- The logic strength is an integer value between 1 and some user-specified upper limit. The upper limit has a maximum allowed value of 65,536. In this report, the subscripts  $f, s$  and  $z$  will be used to denote the largest, middle and smallest strengths respectively in a given range. The strength field is extracted from the state using the "str" function. That is,

$$S = \text{str}(\text{state})$$

- An initial unknown,  $X_i$ , must be distinguished from a unknown generated during the analysis,  $X_g$ . This is done in SPLICE1.6 by defining the initial unknown as follows :

$$X = \text{lev}(\text{initial\_unknown})$$

$$0 = \text{str}(\text{initial\_unknown})$$

and the generated unknown as follows:

$$X = \text{lev}(\text{generated\_unknown})$$

$$0 \neq \text{str}(\text{generated\_unknown})$$

The initial unknown is useful to identify nodes which are not exercised by the input pattern used in a simulation. As a post-processing step, these nodes could be reported to the user.

### 3.2.3. Using the State Model

In a logic analysis, nodes are scheduled to be processed in the time queue in accordance with the activity in the circuit. When a node is

processed, the fanin list (FIL) is obtained from the node data structure (see Appendix II, parts 1,2). Each gate in the fanin list is a potential driver of the node (by definition) but usually only one gate will gain control of the node and determine its final state. The gate with the largest output strength is declared the "winner" and the node adopts the output state of the winning gate. Node contention occurs when two or more gates attempt to drive the same node to different logic levels with the same driving strength. In this case, the node is assigned an X level and the driving strength of any one of the contending gates. The processing details are presented in Section 1.6.

### **3.3. The Delay Model**

#### **3.3.1. Factors Affecting Switching Delay**

Once a new state is determined, the next task is to calculate the time required to reach the new state. In MOS circuits, the switching time is based on many factors which include:

- the basic gate switching time (unloaded)
- the static output loading due to capacitance of elements connected to the node
- the dynamic output loading through transfer gates which are turned "ON" (that is, transistors with their gates at the logic "1" level)
- the number of gate inputs
- the shape (rise and fall times) of input waveforms

No logic simulator attempts to incorporate all of the above factors into the delay calculation. On the other hand, it is essential that a logic simulator

include all the first-order effects in the delay calculation. SPLICE1.6 is capable of handling the first four factors. The fifth factor (input waveform shape) is more difficult to handle at the logic level and is usually considered a second-order effect.

### 3.3.2. Delay Model for Simple Gates

The usual modeling procedure for logic simulation is to generate a set of curves similar to Fig. 3.2 for every primitive element (NANDs, NORs, inverters, etc.) using accurate electrical simulation. In this figure, the delay from the input switching point to the output switching point is plotted as a function of output loading and the number of inputs. Although not strictly true, the relationships are taken to be linear. The y-intercept of each curve represents the intrinsic unloaded gate delay while the slope of each curve represents the gate drive-capability.

Assuming that the above information is available, the following method can be used to calculate delays for simple gates. The first requirement is that a capacitance value be specified on every input and output pin of every gate as part of the model definition. Then the total gate delay can be represented by four parameters : the intrinsic gate delays ( $t_r$ ,  $t_f$ ) and the gate drive-capabilities ( $t_{rc}$ ,  $t_{fc}$ ), where

$t_r$  = rise time for unloaded gate (intercept)

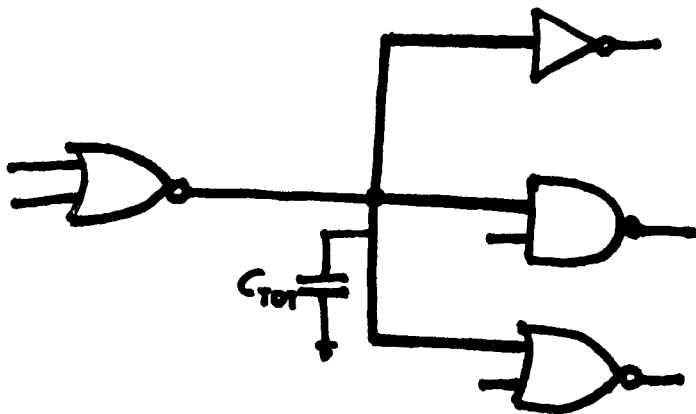
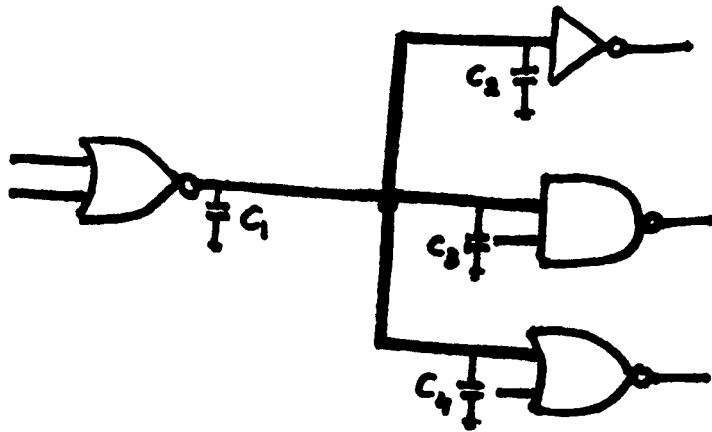
$t_f$  = fall time for unloaded gate (intercept)

$t_{rc}$  = gate drive-capability for rising signals (slope)

$t_{fc}$  = gate drive-capability for falling signals (slope)

Using these values, the total delay is calculated using the equation:

Figure 3.3 : Node capacitance pre-processing



$$C_{TOT} = C_1 + C_2 + C_3 + C_4$$

$$\text{risetime} = tr + trc * (\text{node capacitance}) \quad (3-1a)$$

$$\text{falltime} = tf + tfc * (\text{node capacitance}) \quad (3-1b)$$

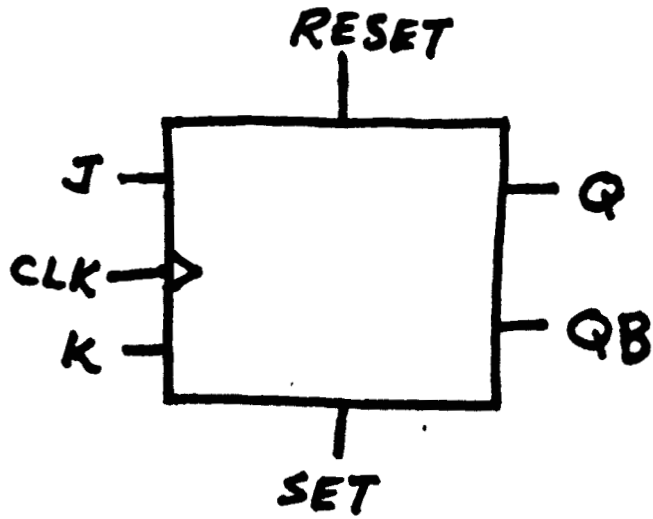
The node capacitance value is extracted in a pre-processing step by summing the capacitances of all elements connected to a node, and stored with the node data structure (see APPENDIX II, part 1). This process is illustrated in Fig 3.3.

### 3.3.3. Delay Model for Multi-output Elements

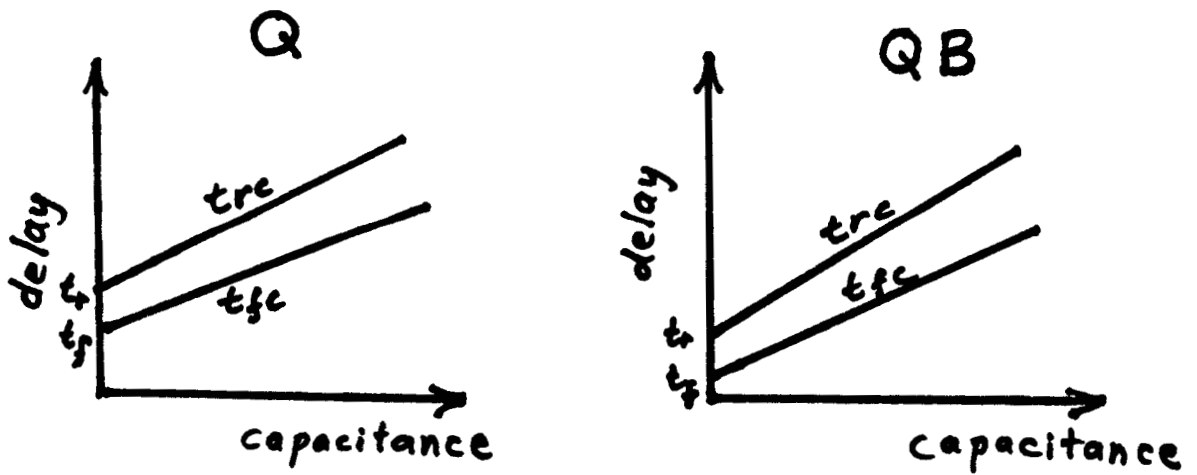
If a multi-output element, such as the flip-flop shown in Fig. 3.4(a), is available as a primitive logic element, each output would have its own set of curves similar to Fig 3.2. The curves for the Q and QB outputs of the flip-flop are shown in Fig. 3.4(b). Then  $4N$  parameters would be required to specify the delay, where  $N$  is the number of outputs. For the flip-flop there would be 8 such parameters : Qtr, Qtf, QBtr, QBtf, Qtrc, Qtfc, QBtrc, and QBtfc. These parameters would be applied to Eqn. (3-1) to calculate the delay. Using this technique, the delay associated with each output could be handled independently. The overriding assumption is that the rise and fall drive-capabilities (trc,tfc) of the outputs are constant and independent of the inputs.

In some elements, the delay from a particular input (say, the RESET pin of the flip-flop) to some output (either Q or QB) is different from another input to output delay (J- or K-input to output delay). This suggests that, in fact, the intrinsic delay should be a matrix which is indexed by input pin which initiates activity and the output pin being processed. Then the total delay due to loading could be calculated using Eqn. (3-1) and the specific trc and tfc values for each output. This is shown in Table 3.1 below for the flip-flop example.

Figure 3.4 : JK Flip-flop Circuit



(a)



(b)

Table 3.1 Intrinsic Delay Matrix

I/O pin	J	K	CLK	RESET	SET
Q	tr=10 tf=10	tr=10 tf=10	tr=10 tf=10	tr=5 tf=6	tr=5 tf=6
QB	tr=10 tf=11	tr=10 tf=11	tr=10 tf=11	tr=5 tf=6	tr=5 tf=6

### 3.3.4. Delay Models for Transfer Gates

The delay calculation for logic circuits containing transfer gates is more complex than either of the two cases given above. Consider the circuit of Fig. 3.5. The delay from Node A to Node B when the input CLK of the transfer gate makes a transition from "0" to "1" is based on:

- the W/L ratio of the transfer gate
- the drive-capability of gate INV
- charge-sharing between C1 and C2

It is a highly non-linear situation and therefore difficult to model in logic. Charge-sharing cannot be represented properly because of the voltage resolution. One way to handle it is by allowing multiple voltage levels similar to the way that the three impedance levels have been extended. This would facilitate the characterization of charge-sharing but would complicate the simulator. The simulator would have to handle transitions from one voltage level to another in a consistent manner. SPLICE1.6 lumps all the non-linear effects into two values called the turn-on (ton) and turn-off (toff) times. These values do not take capacitive effects into account.

Another delay modeling issue concerns transfer gates connected in series as shown in Fig. 3.6. The delay in question is that from Node A to Node E. If all gates are "ON", the circuit can be represented by an RC transmission line. Unfortunately, this is difficult to model at the logic level. A few alterna-

Figure 3.5 : Non-linear Effects due to Transfer Gates

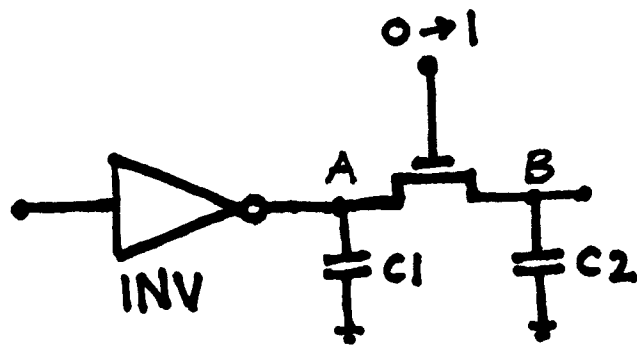
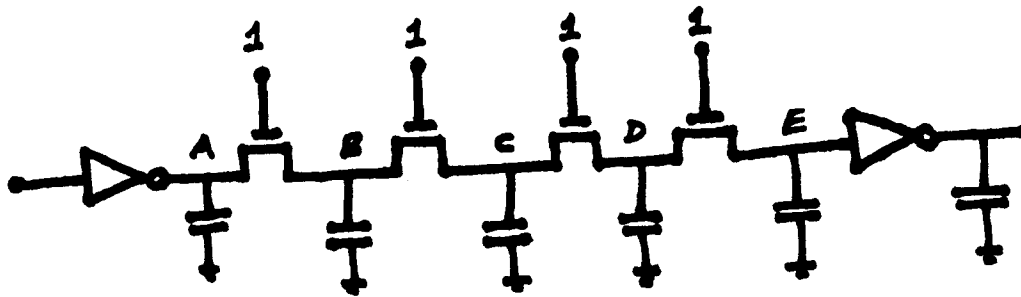


Figure 3.6 : Delay modeling for series-connected MOS Transfer Gates



tives exist to handle this situation:

- Use a zero delay model across transfer gates when they are "ON" [8] . This is the method used in SPLICE1.6. Unfortunately, the value of delay calculated this way is too optimistic at Node E.
- Lump capacitances C1, C2, C3, C4 and C5 together and use this value in eq. (3-1). This is the transition delay for all nodes from the old state to the new one. The value of delay calculated this way is too pessimistic at Node A.
- Extend the notion of drive-capability of a gate to nodes other than its output node. Since tx1 is "ON", both Node A and Node B are driven by gate INV. Therefore, the delay to A could be calculated as given in eq. (3-1) and the delay to B could be calculated using the equation:

$$risetime = trc_{INV} * (capacitance \ at \ B) \quad (3-2a)$$

$$falltime = tfc_{INV} * (capacitance \ at \ B) \quad (3-2b)$$

To compute the delay to nodes C, D and E, simply apply eq. (3-2) again using the capacitance at node C, D and E respectively. This approach is better than either of the above methods but is still lacking in accuracy because it does not account for the "ON" resistance of the transistors. One modification which may provide more accuracy is to adjust the values of trc and tfc using the "ON" resistance of the transfer gates and the depth of the node away from the output of the controlling node. This method is promising because VLSI circuits typically contain interconnections which are electrically equivalent to distributed RC transmission lines. They could be handled exactly the same way as the set of series transfer gates. Therefore, a netlist extractor could provide the simulator with "DELAY" elements, as shown in Fig 3.7, in place of interconnect

with delay calculations performed using the modified eq. (3-2) :

$$\text{risetime} = TRC * (\text{capacitance at node}) \quad (3-3a)$$

$$\text{falltime} = TFC * (\text{capacitance at node}) \quad (3-3b)$$

where

$$TRC = trc * f(\text{resistance, depth})$$

$$TFC = tfc * f(\text{resistance, depth})$$

### 3.3.5. Delay to an Unknown Value

The delay calculations in the previous section assume signal transitions from "0" to "1" or "1" to "0". Nodes may, of course, acquire the X level due to contention at the node as described in an earlier section. The question then arises as to when the X level takes effect. The unknown level could be "0", "1" or some intermediate value. Clearly, if the unknown is the previous value, there is no delay. If it is the opposite logic level there is a rise or fall transition delay. The usual approach is to assume that the unknown value takes affect immediately (as is done in SPLICE1.6) or one time unit in the future.

### 3.4. Spike Handling

SPLICE1.6 uses an inertial delay algorithm. This means that if a node is scheduled to change at some time in the future  $T_n$ , it is held at its old value until that time. Then at  $T_n$ , the new value is assigned to the node and the fanouts of the node are processed using this value. A *spike* (commonly referred to as a glitch) occurs if the node is scheduled to change to a different value before it reaches the new value. Spike detection is simple in true-value logic simulation but becomes very complicated when performing fault simulation. When a spike is detected, the event at  $T_n$  is dropped, the

Figure 3.7 : Equivalent Model for Delay Elements

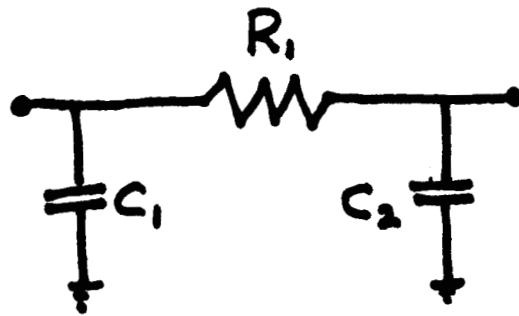
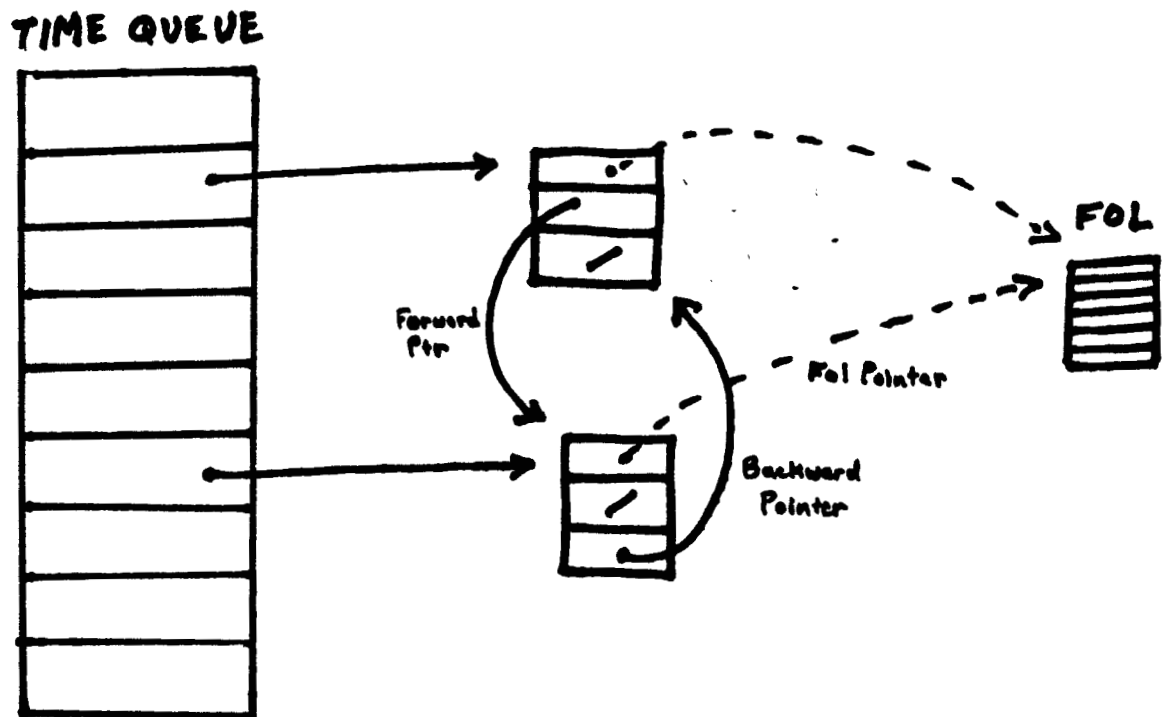


Figure 3.8 : Data Structure for multiple FOL scheduling



new event is scheduled at the appropriate time and the user is notified of the glitch. The glitch is not propagated because it usually signifies an error in the circuit design. Therefore, the simulation will continue as if an error did not occur and more meaningful information may be obtained about the correct operation of circuit. This technique also reduces the amount of work the simulator is required to do because spikes represent activity in the circuit. Therefore, the overall CPU-time will be kept to a minimum by removing glitches from the simulation.

In SPLICE1.6, a fanout list (FOL) can only appear once on the time queue at any given time during the processing. This is a limitation for proper glitch handling, as will be seen in the psuedo-code description of glitch handling which follows. Two different problems are identified which are direct results of the scheduling limitation.

```
#GLITCH HANDLER IN SPLICE1.6
PT = present time
Tnext = next time FOL is scheduled
Tlast = last time FOL was scheduled to be processed
        (or was actually processed)
if (Tlast < PT) { #node was processed in the past
    store new_state ;
    schedule FOL at Tnext ;
}
else if (Tlast = PT) { #node is scheduled now
    if (Tnext ≥ Tlast) {
        if (FOL processed) { # PROBLEM : glitch has been propagated
            update new_state ;
            schedule FOL at Tnext ;
        }
        else { #FOL has not been processed
            #PROBLEM : cannot schedule FOL more than once
            drop schedule at Tlast ;
            replace new_state ;
            schedule FOL at Tnext ;
        }
    }
}
else if (Tlast > PT) { #node is scheduled in the future
    if (Tnext < Tlast) {
        #reschedule time is earlier than originally scheduled time
        report glitch ;
        drop schedule at Tlast ;
    }
}
```

```

        replace new_state ;
        schedule FOL at  $T_{next}$  ;
    }
    else if ( $T_{next} = T_{last}$ ) {
        report glitch ;
        replace new_state ;
    }
    else if ( $T_{next} > T_{last}$ ) { #want to sched in future
        report glitch ;
        drop schedule at  $T_{last}$  ;
        store new_state ;
        schedule FOL at  $T_{next}$  ;
    }
}

```

The problems identified above can be summarized as follows: depending on the order in which nodes are processed at a timepoint, the program may or may not propagate the glitch. Therefore, the output of the simulation depends on the order in which the circuit was specified by the user. The glitch is always identified but its propagation is based on node processing order. One way to get around this problem is to use a two-pass approach by first performing a *leveling* operation [28] as a preprocessing step. This simply means that each node should be assigned a value based on its depth from the inputs. Then every node scheduled at a given timepoint should be processed in *ascending* order. This would incur some overhead but would produce the desired results, i.e., the same solution regardless of the order of the input description. At the present time, SPLICE1.6 will identify the glitch and may or may not propagate the glitch depending on the order the nodes are processed.

Another way to eliminate the problem is by modifying the scheduler data structure so that multiple schedules are allowed. Instead of scheduling FOLs, it would be better to schedule structures which point to the FOL. This structure would have to include other information such as the schedule time, and forward and backward pointers to the next and previous schedules of the

same FOL in the time queue. This would allow easy access to all the schedules of a single FOL for adding and dropping subsequent events. This proposed data structure is shown in Fig. 3.8. One advantage of multiple scheduling is that the program can be modified to perform parallel fault simulation using this data structure.

A simple circuit which is useful for debugging glitch handling code is the clock generator shown in Fig. 3.9. By adjusting  $t_r$  and  $t_f$  for each gate, all possible glitch conditions can be produced. For example, if  $t_r = t_f = 10ns$ , then the glitch problems cited above are generated.

### **3.5. Transfer Gate Modeling Issues**

The incorporation of strengths into the state model does not in itself solve all the problems of MOS logic simulation. As described in the previous section, delay modeling is still difficult and the notion of strengths does not provide any leverage in solving the problem. Transfer gates complicate the situation even more because they introduce dynamic loading effects, bidirectional signal flow, node decay, and charge-sharing. In the sections to follow, these and other problems concerning the transfer gate are described and the solutions used in SPLICE1.6 are presented.

#### **3.5.1. Bidirectional Transfer Gates**

In general, the transfer gate is a bi-directional element but it is usually found in a unidirectional application. That is, the designer intended signals to flow in one direction through the device. SPLICE1.6 provides unidirectional transfer gates (UTXG) for this purpose, as it simplifies the processing thereby reducing CPU-time.

Figure 3.9 : Circuit used to generate all possible Glitch conditions

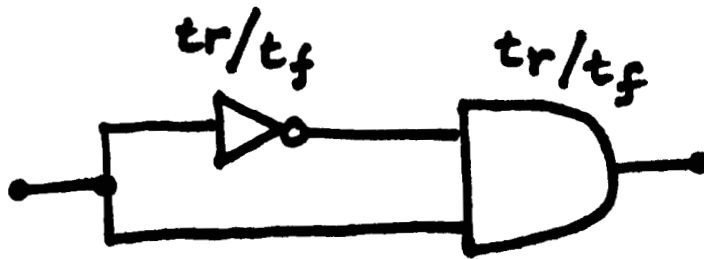
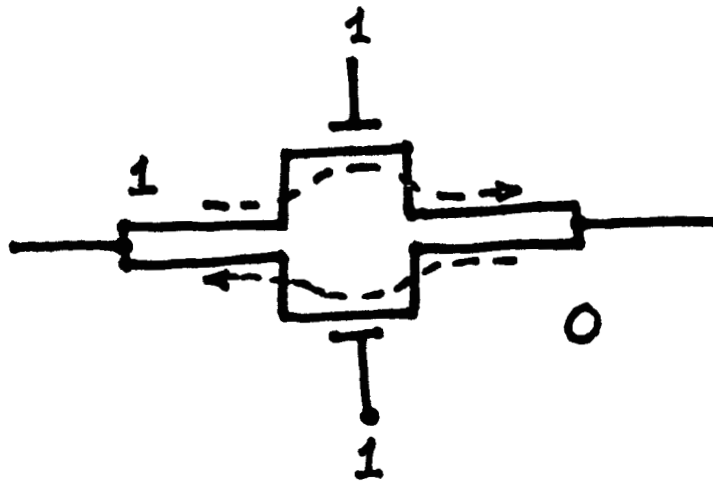


Figure 3.10 : A bi-directional Transfer Gate Model



On the other hand, there are occasions when transfer gates are used in a bidirectional application and therefore the logic simulator must be able to handle them. There have been a variety of modeling approaches for bidirectional transfer gates (BTXG), including the conventional approach of two unidirectional elements back-to-back as shown in Fig. 3.10. This approach can lead to inconsistencies when different logic values are on opposite sides of the element, as is the case in Fig. 3.10. Each value can flow through the BTXG and reach the opposite side and these errors can percolate further through the circuit producing incorrect results. There are ways to get around this problem but they can be very complicated. One way to handle BTXG's in a consistent way is to introduce the concept of composite node relaxation (CNR). In this method, every node connected through transfer gates which are "ON" are considered to be the same node for processing purposes. All fanin lists for the composite node are combined into one list and a new state is determined based on the composite fanin list. Since all nodes connected by "ON" BTXG's are considered the same node, there is no delay between them.

### 3.5.2. Unknowns at Gate Inputs

Another problem in modeling transfer gates is handling unknowns at gate inputs. The problem is identified in Fig. 3.11. Normally, if the transfer gate is "ON" and then shuts "OFF", the output Node A retains its previous value but is reduced in strength (goes to the  $z$  strength). This is shown in Fig. 3.11(a). There are three cases to consider in conjunction with unknowns at transfer gates.

**CASE 1** : Fig. 3.11(b) indicates the situation at the beginning of the simula-

tion. Virtually all gate inputs, except for the ones that have been initialized explicitly, are in the initial unknown condition. In this situation, the gate may or may not pass signals.

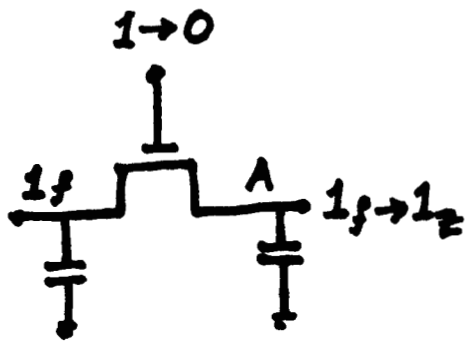
**CASE 2 :** The second situation occurs when there is a logic "1" at the input and it becomes a logic "X". In this case, the level at the output remains the same but the strength is not known. This is illustrated in Fig. 3.11(c).

**CASE 3 :** The third situation is the reverse of the second. Here, the input goes from logic "0" to logic "X". Both the value and strength may change. This is shown in Fig. 3.11(d).

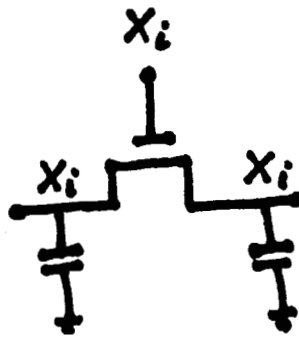
There are a few alternative methods to handle unknowns at gate inputs.

- (1) a pessimistic approach is to generate  $X_f$  at the output so that it will be propagated further. This may produce incorrect circuit operation if CASE 2 is considered, but is the easiest to implement.
- (2) another approach is to have the notion of unknown strengths. Using this model, CASE 2 could be handled by setting the output node to its previous value with an unknown strength. This introduces some complications in the way the simulator processes nodes. Some bit pattern would have to be selected for unknown strengths. It is not clear how this special strength value would interact with other strengths.
- (3) assume that devices are "CN" and process nodes. Then turn devices "OFF" and reprocess nodes. If conflicts result at any nodes, then set them to "X". If no conflicts occur, then set nodes to correct level and a pessimistic strength [29].

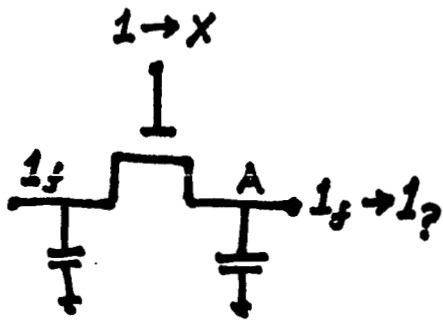
Currently, method (1) is used in SPLICE1.6 and methods (2) and (3) are being investigated further.



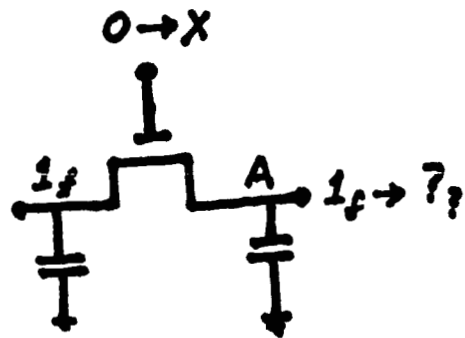
(a)



(b) CASE 1



(c) CASE 2



(d) CASE 3

Figure 3.11 : Handling Unknowns at gate inputs

### 3.5.3. Node Decay

When a node acquires the  $z$  strength, it retains the previous state on the capacitance at the node. Physically, charge is trapped at the node and there are parasitic resistive paths from the node to ground or VDD. Therefore, the node will eventually lose its value and it will become unknown. This is referred to as *node decay*. The time constant for the decay is large but finite.

It is useful to include node decay as part of the simulation, especially for dynamic circuits. One way to do this is to detect the  $z$  strength at a node and schedule the node to decay after a specified amount of time by setting a special flag at the node. If the node is not refreshed before this time, the node is placed in the unknown state. If the node is redriven, the scheduled event would be dropped and processing would continue. Unfortunately, the program would incur an excessive amount of scheduling and de-scheduling overhead, especially in the case of dynamic MOS circuits. Moreover, in SPLICE1.6, most of the scheduled nodes would be put into the pool (see Appendix II, part 5). The pool is an overflow area designed to handle all schedules which are greater than 200 timepoints in the future. This would always be the case for node decay. Clearly this is not a suitable approach.

An alternative approach, proposed by Boyle [30], is to simply store the decay time along with the node data structure and avoid scheduling altogether. Everytime the node is redriven, this value could be compared to the current time. If the current time is greater than the decay time, a warning message could be sent to a file if the user has requested it. Then processing would continue as if node decay had not occurred. It is not useful to simulate the circuit under decay conditions because it is usually a design error.

Therefore, as was done in glitch handling, it is simply flagged as an error and then ignored for the remainder of the simulation.

### 3.6. Logic Simulation Implementation Details

#### 3.6.1. General Program Flow

The following is a high-level psuedo-code description of the general program flow during a logic analysis. Note the parallel between the ITA program flow described in the previous chapter and the code below:

```

set all nodes to their initial values ;
schedule all FOL's at time 0 ; # FOL = fanout list
 $t_n = 0$  ;
while (  $t_n \leq TSTOP$  ) {
  for (each FOL in the queue at the current timepoint) {
    for (each element in the FOL) {
      for (each output node of an element) {
        process node ; #see next section for details
        schedule FOL if necessary ;
      }
    }
  }
  plot all active nodes ;
   $t_n \leftarrow t_{n+1}$  ;
}

```

### 3.6.2. Node Processing Details

```

# LOGIC NODE PROCESSING DETAILS
#
begin
  current_state ← (X,0);
  place node in CNL; # CNL = composite node list
  for (each node in the CNL) {
    for (each element in the FIL) { # FIL = fanin list
      if (element = BTXG) & (gate = "ON") {
        place node in CNL;
      }
      else {
        determine output_state (L,S) of element;
        intend_state ← output_state;
      }
      if ( str(intended_state) > str(current_state) )
        current_state ← intended_state;
      else if ( str(intended_state) = str(current_state) )
        if ( lev(intended_state) ≠ lev(current_state) )
          lev(current_state) ← X;
    }
  }
  new_state ← current_state
  if (new_state ≠ old_state) {
    for (each node in CNL) {
      calculate delay(old_state,new_state);
      call GLITCH HANDLER to schedule FOL; # FOL = fanout list
    }
  }
end

```

### 3.7. Switch-level Simulation

The definition of UTXG and BTXG elements allows a switch-level simulation [9, 10] to be performed using SPLICE1.6. Loads can be modeled using a UTXG with a "soft" output strength. Drivers can be modeled using a UTXG with a "forcing" output strength. Either a BTXG or a UTXG can be used for pass transistors depending on the application. Other floating transistors must be BTXG's. If "ton" and "toff" are specified as 1 unit of time, then a unit-delay switch-level simulation will be performed by SPLICE1.6. An interesting parallel can now be drawn between the electrical and logic simulators in SPLICE1.6. The processing sequence is exactly the same in both

cases. Only the resolution of the voltage levels and the transistor models are different. Unfortunately, there is no timing information in the transistor-level logic simulation. If timing information could somehow be included in a switch-level simulation, then mixed-mode simulation at the transistor would be quite feasible. For obvious reasons, delays at the switch-level cannot be handled the same way as it is currently done in SPLICE1.6 for standard boolean gates. Three approaches have been proposed to introduce timing information at the switch-level [31, 32, 29] using a resistive simulation model. These methods are under investigation at the present time.

## CHAPTER 4

### 4. Examples and Results

This chapter presents a number of simulation results and program performance statistics of SPLICE1.6. Five aspects of the program are examined in the sections to follow. These are :

- the program performance statistics such as processing speed for electrical and logic nodes, typical storage requirements per element, iteration counts ,etc.
- the identification of bottlenecks using profilers
- the factors which affect the run-times such as **mindvsch**, **sor**, **mrt** and floating capacitors
- SPLICE1/SPICE2 comparisons for execution speed and memory requirements
- the program's ability to handle analog circuits

The simulations were carried out using two large digital circuits, one small analog circuit and one small digital circuit. They were as follows:

- (1) **Digital Filter Circuit** : This circuit was obtained from[1] . It is an integrated circuit which performs a digital filtering function. There are 705 MOS transistors and 393 nodes in the circuit. The simulation period is  $4\mu s$ .
- (2) **Counter-Decoder-Encoder Circuit** : This circuit is a combination of a 4-bit counter driving a 4:16 decoder and a 16:4 encoder. It will be referred to as the CDE circuit in the rest of the chapter. The switching

times were based on the specifications provided in a TTL Handbook [33]. The circuit has 1,326 MOS transistors and 553 nodes. The simulation period is also  $4\mu\text{s}$ [34].

- (3) **NMOS Operational Amplifier** : This circuit was obtained from [35]. It was used as part of a phase-locked loop circuit. Fig. 4.4(a) is a schematic diagram of the MOS operational amplifier (opamp). This circuit is used to illustrate the capability of ITA in handling analog circuits.
- (4) **Boot-strapped Inverter Circuit** : This circuit was described earlier in Chap. 2. It is illustrated in Fig. 2.4. The circuit is used to examine the degradation effects of a floating capacitor element in an ITA simulation.

#### 4.1. Program Performance Statistics

In order to predict the run-times and memory requirements of the program SPLICE1.6, the program execution speed and memory usage statistics are required. These statistics have been tabulated below for both the electrical and logic simulators.

##### Electrical Simulation Statistics

Node Evaluations	600 nodes/sec.
SOR-Newton Iterations (no floating caps)	3-5 iterations/node
SOR-Newton Iterations (with floating caps)	6-20 iterations/node

##### Electrical Element Storage Requirements

Elements	Type	Words Required
Transistors	Load	3 x no. of loads
	Driver	4 x no. of drivers
	Transistor	5 x no. of transistors
Capacitors	Grounded	0
	Floating	3 x no. of capacitors

Resistors		3 x no. of resistors
<b>Element Model</b>	<b>Type</b>	<b>Words Required</b>
Transistors	Load	11 x no. of loads
	Driver	11 x no. of drivers
	Transistor	12 x no. of transistors
Capacitors	Grounded	1 x no. of grounded capacitors
	Floating	3 x no. of floating capacitors
Resistors		3 x no. of resistors

**Logic Simulation Statistics**

Node Evaluations 650 nodes/sec.

**Logic Element Storage Requirements**

Elements	Words Required
inverter	3 x no. of inverters
buffer	3 x no. of buffers
AND	~5 x no. of ANDs
OR	~5 x no. of ORs
NAND	~5 x no. of NANDs
NOR	~5 x no. of NORs
XOR	~5 x no. of XORs
XNOR	~5 x no. of XNORs
transfer gates	~4 x no. of devices

Model Type	Words Required
inverter	11 x no. of different inverter models
buffer	11 x no. of different inverter models
AND	~ 11 x no. of different AND models
OR	~ 11 x no. of different OR models
NAND	~ 11 x no. of different NAND models
NOR	~ 11 x no. of different NOR models
XOR	~ 11 x no. of different XOR models
XNOR	~ 11 x no. of different XNOR models
transfer gates	~8 x no. of device models

**Node Storage Requirements**

$N$  = number of circuit nodes

Data	Logic Node	Electrical Node
------	------------	-----------------

Node list	1	1
Node pointers	N	N
Node data	8N	9N
Node FIL	N	3N
Node FOL	3N	3N
Capacitor	N	N

#### 4.2. Profile Statistics

The SPLICE1.6 program execution times can be reduced by applying some of the techniques suggested in Chap. 2, based on intuitive arguments. On the other hand, it is useful to monitor the program during execution using "profilers" to determine exactly where the program is spending most of its time. Using this information, the program can be modified in sections where it will provide the most benefit.

The following profile statistics were obtained from a simulation of the digital filter circuit using electrical analysis.

total time: 3196 seconds

time(%)	time(sec.)	no. of calls	name	subroutine task
28.7	916.33	1222883	prtim	processing a timing node
17.3	554.47	2449814	intxg	evaluate transistor model
14.2	455.32	5799795	getexv	get a value from another node
8.2	231.63	951895	sqrt	perform a square root operation
6.3	203.63	900167	tndri	evaluate driver model
5.1	164.07	658140	tnloa	evaluate load model
4.7	152.62	792936	prelm	process an element in the FOL
1.6	51.92	4001	prfot	process a FOL in the time queue
1.3	40.23	276985	adsfo	add a FOL to the time queue
1.2	37.53	24046	dropf	drop a FOL from the time queue
0.3	9.70	20547	prout	print out a node

It is clear that most of the time is spent processing nodes and evaluating transistor models for the SOR-Newton iteration. Therefore, any speed-up techniques should be applied to these areas of the program rather than FOL

processing, node printing, etc.

### 4.3. Factors Affecting Execution Time in Electrical Simulation

#### 4.3.1. CPU-time vs. MRT

SPLICE1.6 has a user-specified fixed simulation timestep called the **mrt** (Minimum Resolvable Time). The symbol  $h$  will be used to refer to the timestep associated with a particular node. In SPLICE1,  $h$  is some integer multiple of **mrt**. Although the simulation timestep is fixed, the value of  $h$  for a specific node is dependent on the activity at that node. For example, when the node is active,  $h$  is equal to **mrt**. Otherwise,  $h$  is defined by the time difference between two events at the node. In a sense, the timestep at a node is determined implicitly by the activity in the circuit.

Since there is no explicit dynamic timestep control in the SPLICE1, the CPU-time required to perform an electrical simulation is dependent on the value chosen for **mrt**. Fig. 4.1 illustrates this relationship for the CDE circuit. There is a definite optimum value of **mrt** for this particular circuit and this holds true in the general case. At values of **mrt** greater than the optimum value, there are two effects occurring simultaneously :

- the diagonal dominance condition of the conductance matrix is weakened by the fact that the  $\frac{C}{h}$  terms in the diagonal are smaller; therefore, the program will iterate longer to obtain a consistent solution ;
- the difference between the solution at a time  $t_n$  and  $t_{n+1}$  increases as **mrt** increased and so the Newton-Raphson convergence rate may be linear instead of quadratic.

Figure 4.1 :  
CPU-time vs mrt

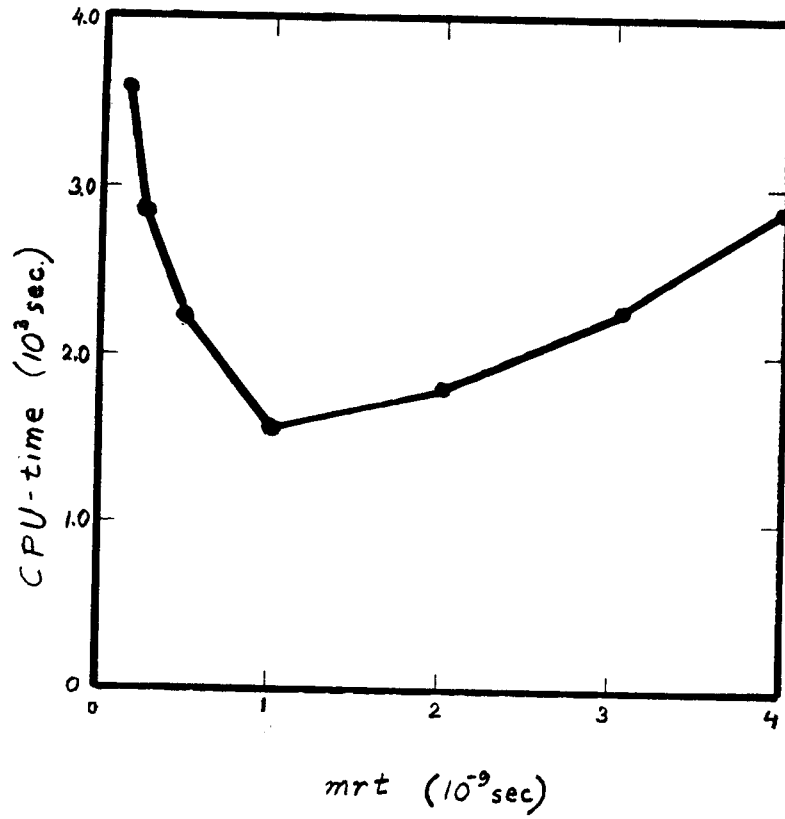
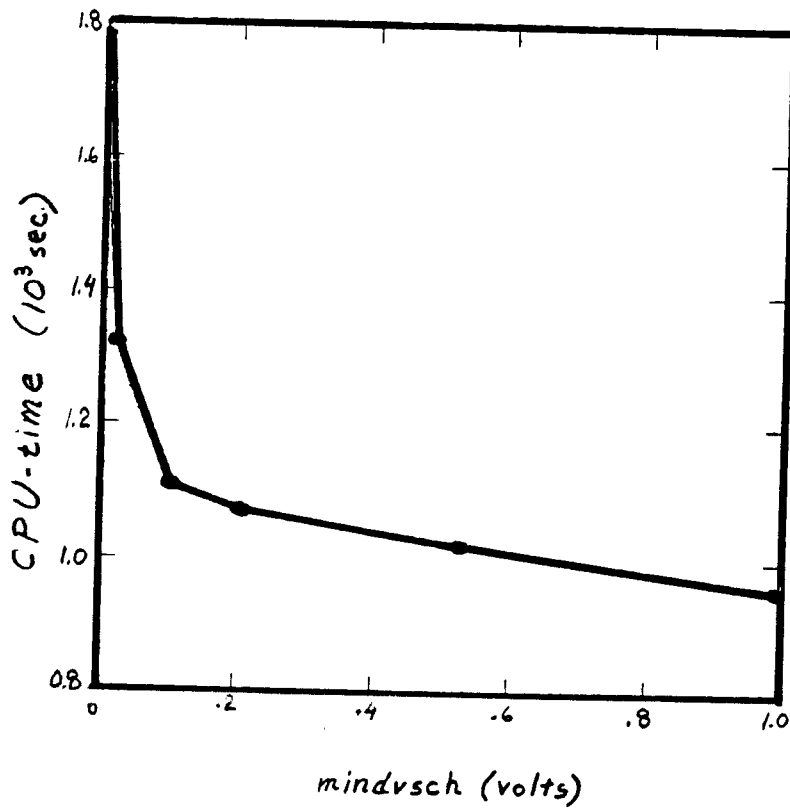


Figure 4.2 :  
CPU-time vs. mindvsch



At **mrt** values less than the optimum, the program is forced to do more work during the active periods than is really necessary, based on the time constants in the circuit. Therefore, there is a rapid rise in the curve in Fig. 4.1 at small values of **mrt**. It has been observed that at very small timesteps, the curve begins to level off. This is probably due to the fact that the prediction step is very accurate and only one or two iterations are required for convergence.

The relation between CPU-time and **mrt** suggests that, for a given technology, the optimum value should be obtained through experiment and used in all further simulations. Of course, if an explicit dynamic timestep control mechanism is implemented, this would not be necessary.

#### 4.3.2. CPU-time vs. MINDVSCH

In SPLICE1, events at a node are propagated to its fanouts if the change in the node voltage is considered to be significant. If the change is not significant, the fanouts are not scheduled and the node is returned to its original value. This constitutes the event-driven selective-trace feature in SPLICE1. The scheduling threshold parameter, used to determine whether or not the change is significant, is called **mindvsch**. It is specified in units of volts, by the user, for an entire simulation and is the same for every node in the circuit.

The value chosen for **mindvsch** has a profound effect on simulation results. Careful consideration must be given to select an appropriate value for this parameter. It can be thought of as the minimum voltage change which can affect the fanout elements of a node. Therefore, an upper bound for digital circuits is the threshold voltage,  $V_T$ , usually in the order of 1V.

The lower bound on **mindvsch** is the value used to determine convergence at a node, called **abstol**, which is typically  $1\mu V$ . Therefore, a value of **mindvsch** lies in the range from  $1\mu V$  to  $1V$ . Based on experience with the program, an appropriate value for most digital circuits is  $1mV$ .

The effect of **mindvsch** on CPU-time is quite dramatic as shown in Fig. 4.2. As **mindvsch** is increased, the CPU-time goes down. This suggests that the value should be made as large as possible. Unfortunately, some significant events may be accidentally dropped if the **mindvsch** is too large resulting in a loss of accuracy. Also, node voltages can only reach a value which is within **mindvsch** of their final value because the remaining voltage change is not considered significant. Hence, if **mindvsch** is too large, there will be errors at the end of each transition.

#### 4.3.3. Effect of Floating Capacitors

As indicated in Chap. 2, floating capacitors no longer pose a problem to the electrical analysis in terms of accuracy but tend to degrade the simulator performance. The factor which determines the amount of degradation is the ratio of the floating capacitor to the grounded capacitor. In order to illustrate the relationship between CPU-time and capacitance ratio, the boot-strapped inverter of figure 2.4 was simulated with different values of  $\frac{C_{float}}{C_{gnd}}$ . The results have been plotted in Fig. 4.3. It is clear from this graph that there is the relationship obeys a square-root law. This relationship has also been observed for large circuits in which all transistors have parasitic  $C_{gs}$  and  $C_{gd}$  capacitors represented.

Although the graph indicates that solutions may be obtained regardless of the ratio, this is not true in general. Therefore, if the ratio is too large,

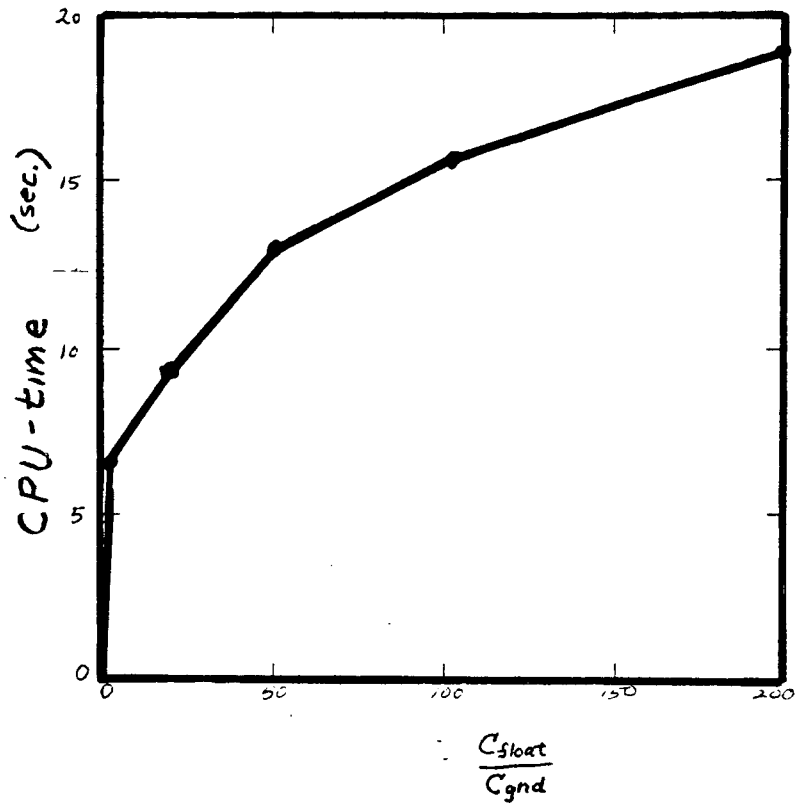


Figure 4.3 :  
CPU-time vs.  
capacitance ratio

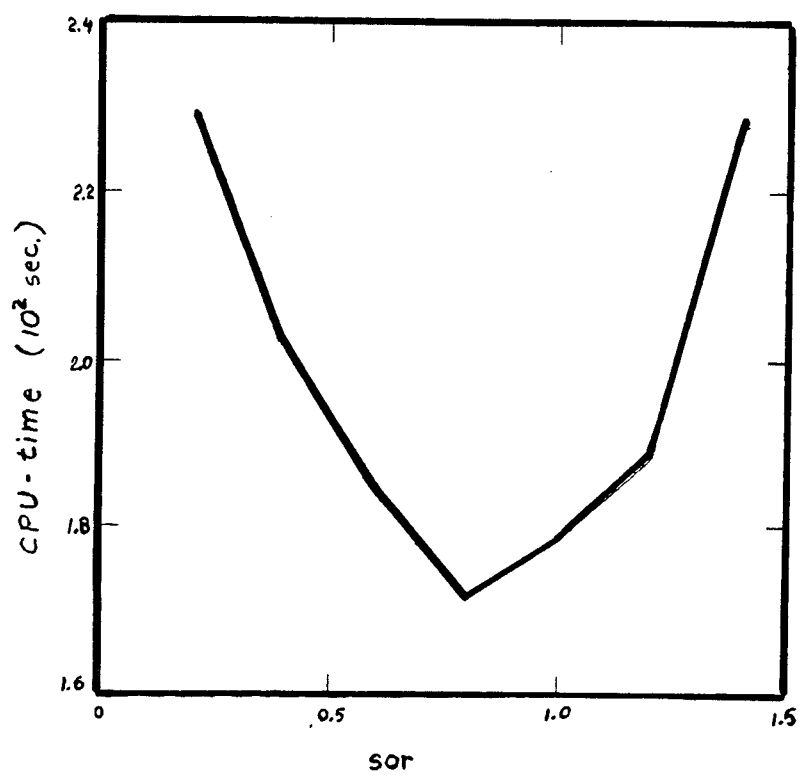


Figure 4.4 :  
CPU-time vs. SOR

the iteration may not converge. Special techniques must be used to reduce the number of iterations required to solve nodes with floating capacitors since this is usually the case. Research is underway to find ways to accomplish this.

#### 4.3.4. CPU-time vs. SOR

The **sor** parameter was introduced in Chap.2 as an acceleration parameter for the non-linear Gauss-Seidel iteration. This parameter has a significant effect on the CPU-time but does not affect simulation accuracy. Fig. 4.4 shows the relationship between CPU-time and **sor** obtained from simulations performed on the digital filter circuit. There is an optimum value of **sor** which minimizes the run-time of the simulation. In this case, the optimum value is 0.8.

Although the optimum value changes from technology to technology, it is worthwhile to obtain the value experimentally as it may provide a substantial improvement over the standard Gauss-Seidel iteration.

#### 4.4. SPICE2 vs. SPLICE1.6

The two large digital circuits were simulated using SPICE2 and SPLICE1.6 for comparative purposes and the results have been placed in Table 4.1. The simulations were performed on a VAX-11/780 running under the UNIX operating system. In the CDE circuit, SPLICE1.6 was 66 times faster than SPICE2 and its memory usage was 35 times smaller. In the digital filter, SPLICE1.6 was 17 times faster and its memory usage was 21 times smaller than SPICE2.

It is clear from these two examples that ITA is much faster than the standard approach for large digital circuits. In fact, as the circuit size

increases, the improvement factor increases. This is due to the fact that the solution time in SPICE2 increases exponentially with the circuit size, as described in Chap. 2, whereas it is approximately linear in SPLICE1.6. If the circuit size is small, the standard approach is usually more efficient.

Circuit Mofets Nodes	CDE		Digital Filter	
	Time (s)	Memory (Kbyte)	Time (s)	Memory (Kbyte)
SPICE2G	115,840	2,420	30,582	1,038
SPLICE1.6	1,740	68.9	1,783	48.4

Table 4.1  
Comparison of conventional circuit simulation,  
and iterated timing analysis for two examples.

#### 4.5. NMOS OpAmp Example

Although ITA was developed for the simulation of large digital circuits, the algorithm is robust enough to accurately simulate complex analog circuits. Therefore, an integrated circuit consisting mainly of digital circuits and a few analog blocks, commonly found in telecommunication circuits and memory chips, can be simulated without any special precautions other than the usual requirement of a grounded capacitor at every node.

The OpAmp in Fig. 4.5 was simulated using SPLICE1.6 and SPICE2. Notice the large floating compensation capacitor. The circuit was connected in a unity-gain configuration and a step voltage was applied at the input. Fig. 4.6 shows the output of SPLICE1.6 and SPICE2. The output of the two simulators are identical except in the neighborhood of time 0 due to slightly different initial conditions assumed by each program. In this particular case, the execution time of SPICE2 was two times faster than SPLICE1.6 because of the size and nature of the circuit. This difference can be reduced

by applying optimizations to the implementation in SPLICE1.6, as described earlier, based on information obtained by profiling programs.

In general, ITA will encounter problems simulating analog circuits, in terms of CPU-time and convergence, because:

- they usually contain strong feedback and high gain paths
- there is little or no latency in a typical analog circuit.

Therefore, the accuracy tolerances on the simulation (**abstol**, **reltol**) must be tight and the scheduling threshold, **mindvsch**, must be very small. There may also be a requirement for a small simulation timestep to guarantee convergence. Therefore, a dynamic timestep control mechanism is almost essential for simulating mixed analog/digital circuits so that the timestep will not be overconstrained by the analog circuits. Another useful feature would be to allow parameters such as **abstol**, **reltol** and **mindvsch** to be specified on a per node basis. Then, certain nodes could be forced to iterate longer than others to ensure accuracy. These and other techniques may be used to improve the simulator performance in handling analog circuits, although ITA may not be ideally suited to the task.

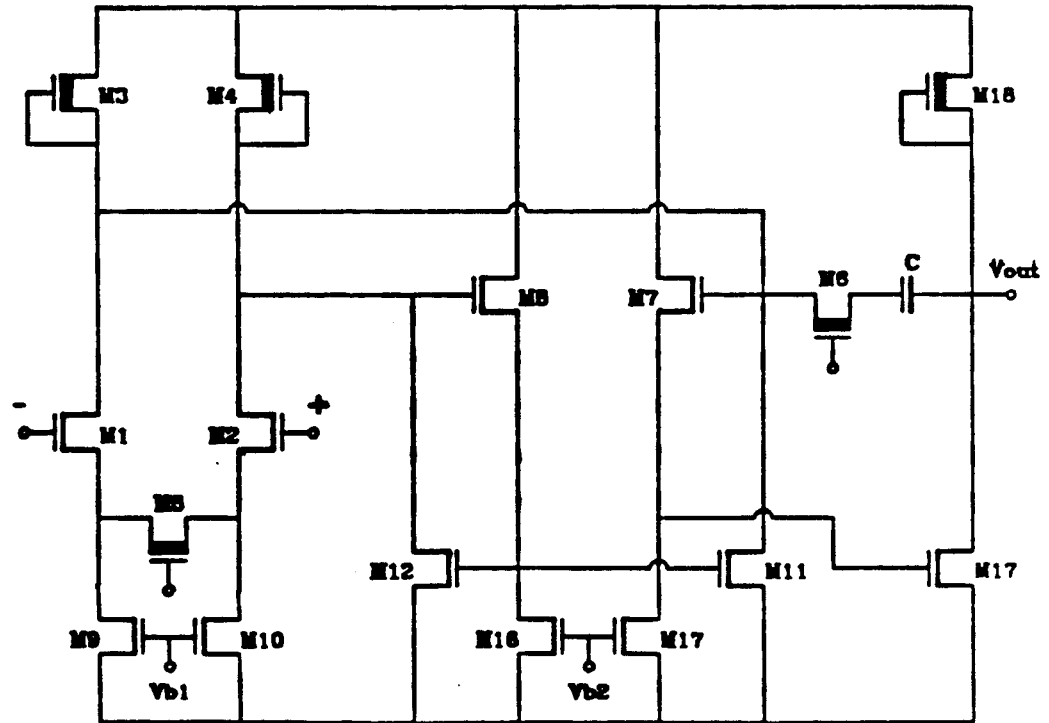
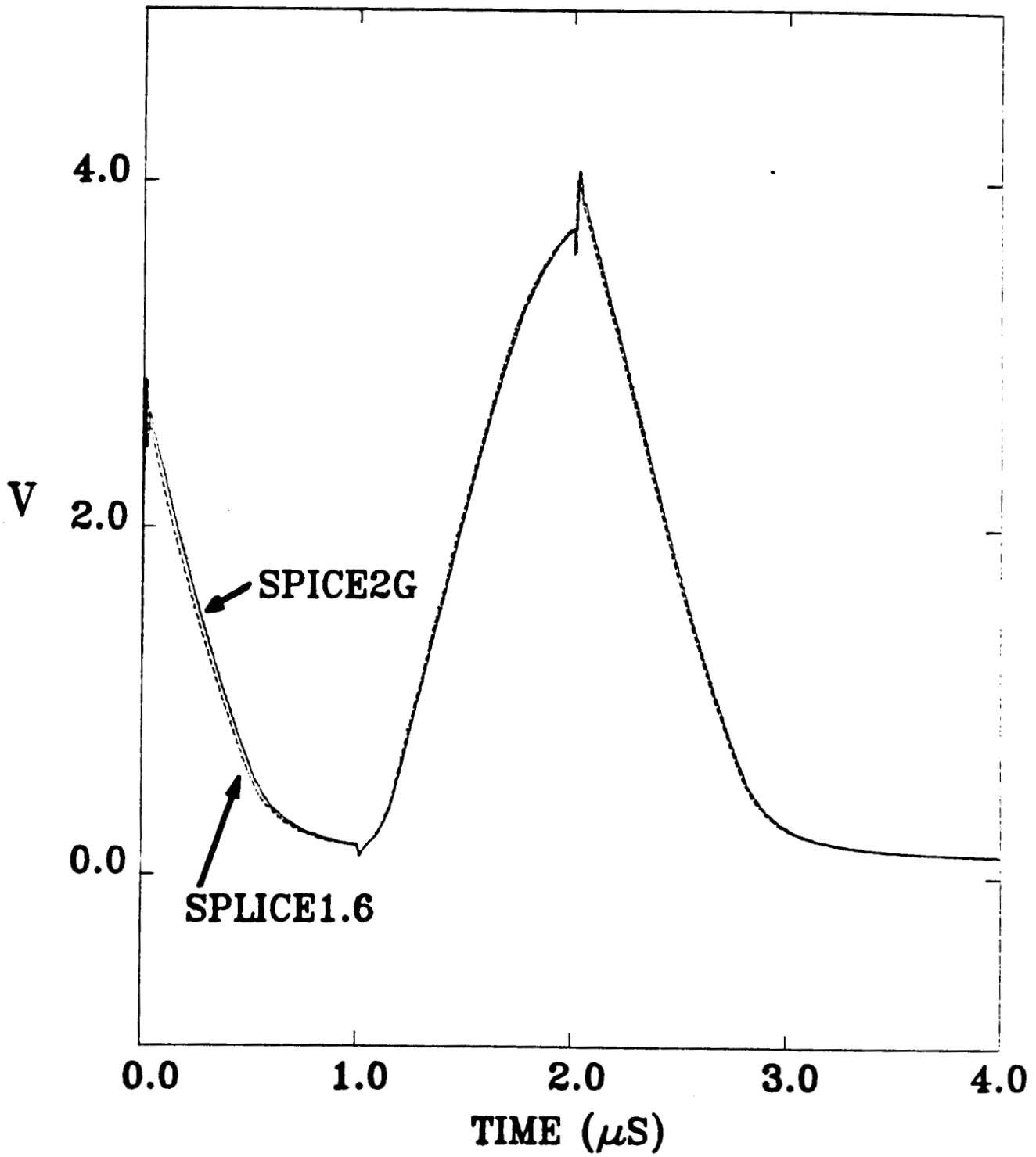


Figure 4.5 : NMOS Operational Amplifier Circuit

Figure 4.6 : Comparison of SPICE2 and SPLICE1.6 for NMOS Operational Amplifier Circuit in Fig. 4.5



## CHAPTER 5

### 5. CONCLUSIONS

SPLICE1.6 has been greatly improved by incorporating the new techniques described in this report. As evidenced by the statistics in Chap. 4, the new electrical simulation approach, ITA, is substantially faster than SPICE2 and requires far less storage. This method has shown so much promise that efforts are underway to generalize it as a standard circuit simulation approach. As pointed out earlier, the major problem with the method is the number of iterations required to obtain a solution when floating capacitors are present in the circuit. As the prototype program is developed further, it is expected that the performance characteristics will be significantly better than SPICE2. The ITA method provides a way to efficiently simulate large digital circuits and it may replace the standard approach in this application. It is also suitable for implementation on special-purpose hardware and work is underway in this area.

The logic analysis in SPLICE1.6 has been enhanced to perform true-value logic simulation using a strength-oriented MOS model. This not only allows accurate modeling at the logic level but also provides a mechanism to perform accurate mixed-mode simulation. There is still work to be done in the area of strength modeling for logic elements so that the electrical/logic interfaces can be defined accurately. SPLICE1.6 handles logic transfer gates in a consistent manner but there are still unanswered questions in the area of delay modeling at the switch-level. Research is currently being directed at applying multiple iterations at the logic level to determine delays.

In conclusion, the concepts presented in this report suggest that mixed-mode electrical and logic simulation is best applied at the transistor-level using relaxation-based algorithms and event-driven selective trace techniques, along with consistent signal representation for accurate conversions from one domain to the other.

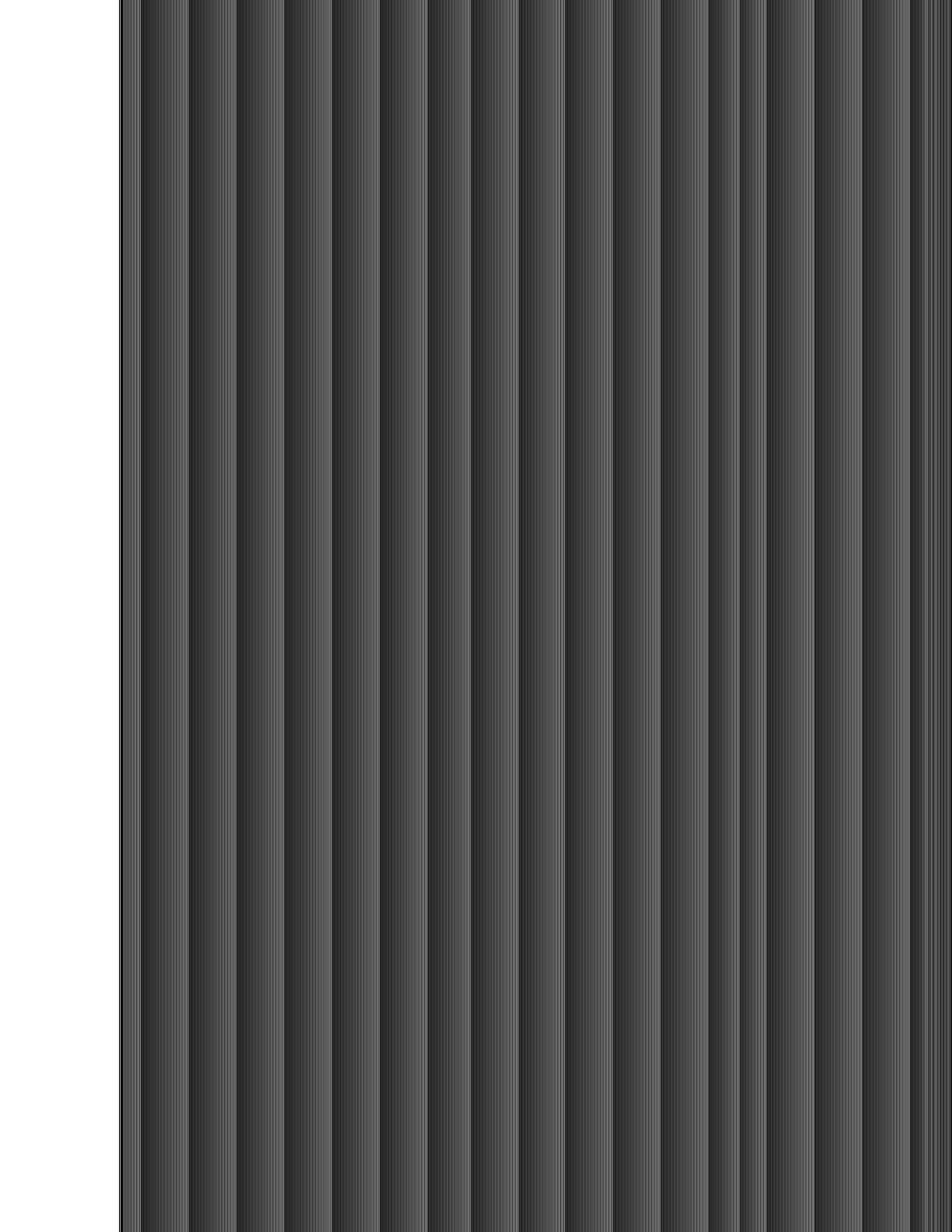
## References

1. A.R. Newton, *The Simulation of Large Scale Integrated Circuits*, University of California, Berkeley (July 1978). Ph.D. Dissertation
2. A.R. Newton, "The simulation of large scale integrated circuits," *IEEE Trans. on Circuits and Systems* Vol. **CAS-26** pp. 741-749 (September 1979).
3. A.R. Newton, "Timing, Logic and Mixed-mode Simulation for Large MOS Integrated Circuits," pp. 175-240 in *Computer Design Aids for VLSI Circuits*, ed. P. Antognetti, D.O. Pederson, and H. De Man, Sijithoff and Noordhoff (1981).
4. B.R. Chawla, H.K. Gummel, and P. Kozak, "MOTIS-an MOS timing simulator," *IEEE Trans. on CAS* Vol. **CAS-22** pp. 901-909 (Dec. 1975).
5. S.P. Fan, M.Y. Hsueh, A.R. Newton, and D.O. Pederson, "MOTIS-C A new circuit simulator for MOS LSI circuits," *Proc. IEEE Int. Symp on Cir. and Syst.*, (April 1977).
6. W. Nagel, "SPICE2, A Computer Program to simulate semiconductor circuits," ERL-M520, University of California, Berkeley, California (May 1975). Ph.D. Dissertation
7. *LOGIS: User's Manual Version 4*, ISD Corporation (1980).
8. F. Jenkins, *ILOGS: User's Manual*, Simutec (1982).
9. R.E. Bryant, "An Algorithm for MOS Logic Simulation," *LAMBDA*, pp. 46-53 (4th Quarter 1980).
10. C.M. Baker and C. Terman, "Tools for Verifying Integrated Circuit Designs," *LAMBDA*, (4th Quarter 1980).

11. J.L. Burns, A.R. Newton, and D.O. Pederson, "Active Device Table Look-up Models For Circuit Simulation," *Proc. 1983 Int. Symp. on Circ and Syst.*, (May 1983).
12. A.R. Newton and A.L. Sangiovanni-Vincentelli, *Relaxation-Based Electrical Simulation*, University of California, Berkeley (1983). To be published.
13. "Advanced statistical analysis program (ASTAP) Program reference manual," Pub. No. SH20-1118-0, IBM Corp. Data Proc. Div., White Plains, NY
14. N. Tanabe, H. Nakamura, and K. Kawakita, "An MOS Circuit Simulator for LSI," *Proc. IEEE Int. Symp. on Circ. and Syst.*, pp. 1035-1039 (April 1980).
15. G.R. Boyle, *Simulation of Integrated Injection Logic*, University of California, Berkeley (March 1978). Ph.D. Dissertation
16. J.M. Ortega and W.C. Rheinboldt, *Iterative Solution of Nonlinear Equations in Several Variables*, Academic Press, New York (1970).
17. K. Sakallah and S.W. Director, "An activity-directed circuit simulation algorithm," *Proc. IEEE Int. Conf. on Circ. and Computers*, (October 1980).
18. E. Cohen, *Performance Limits of Integrated Circuit Simulation on a Dedicated Minicomputer System*, Bell Laboratories internal memorandum (May 1981).
19. A. Vladimirescu and D.O. Pederson, "Performance Limits of the CLASSIE Circuit Simulation Program," *Proceedings of the Int. Symp. on Circ. and Syst.*, (May 1982).

20. E. Lelarasme, A. Ruheli , and A.L. Sangiovanni Vincentelli, "The Waveform Relaxation Method for the Time-Domain Analysis of Large Scale Integrated Circuits," *IEEE Tran. on CAD of Int. Circ. and Sys.* Vol **CAD 1, No. 3** pp. 131-145 (Aug 82).
21. J. White and A. Sangiovanni-Vincentelli, "RELAX2: A New Waveform Relaxation Approach for the Analysis of LSI MOS Circuits," *Proc. 1983 Int. Symp on Circ. and Syst.*, (May 1983).
22. J. E. Kleckner, R. A. Saleh , and A. R. Newton, "Electrical Consistency in Schematic Simulation," *Proc. IEEE Int. Conf. on Circ. and Comp.*, pp. 30-34 (October 1982).
23. R. A. Saleh, J. E. Kleckner, and A. R. Newton, "Iterated Timing Analysis and SPLICE1.6," *Proc. IEEE Int. Conf. on Computer-Aided Design*, (September 1983).
24. L.O. Chua and P.M. Lin, *Computer-Aided Analysis of Electronic Circuits: Algorithms & Computational Techniques*, Prentice-Hall, Inc., Englewood Cliffs, N.J. (1970).
25. A.R. Newton, "The Analysis of Floating Capacitors for Timing Simulation," *Proc. 13th Asilomar Conference on Circuits Systems and Computers*, (November 1979).
26. H. Schichman and D.A. Hodges, "Modeling and Simulation of Insulated Gate Field-Effect Transistor Switching Circuits," *IEEE Journ. on Solid State Circuits* Vol. **SC-3** pp. 285-289 (Sept. 1968).
27. J.E. Kleckner, *Iterated Timing Analysis and SPLICE2*, To be published
28. G.R. Case, "The SALOGS - A CDC 6600 Program to Simulate Digital Logic Networks," Sandia Laboratory Report No. SAND 74-044 (1975).

29. D. Dumlugol, H. De Man, P. Stevens, and G. Schrooten , *Local Relaxation Algorithms for Event Driven Simulation of MOS Networks Including Assignable Delay Modelling*, Katholieke Universiteit Leuven, Belgium ().  
To be published.
30. Graeme Boyle, Private communication.
31. Gregory D Jordan and Ravi M. Apte, "Modeling of MOS Transistors in a Logic Simulator," *Proc. IEEE Int. Conf. on Circ. and Comp.*, pp. 431-434 (October 1982).
32. C.J. Terman, *Simulation Tools for Digital LSI Design*, Massachusetts Institute of Technology (December 1981). Proposal for Ph.D. Research
33. , *The TTL Data Book for Design Engineers - 2nd Edition*, Texas Instrument Incorporated (1976).
34. Jim Kleckner constructed the CDE circuit.
35. D. Senderowicz, *An NMOS Integrated Vector-Locked Loop*, University of California, Berkeley (Nov. 1982).



**APPENDIX I**

**SPLICE1.6 User's Guide**



## **APPENDIX II**

### **SPLICE1.6 Data Structures**



## APPENDIX II

### SPLICE1.6 Data Structures

- (1) **Nodes:** The node data structure is set up in GENFS for the logic, electrical and vrail nodes.

**LOGIC NODE :**

offset	abbrev.	definition
0	fop	fanout pointer
1	fip	fanin pointer
2	type	=1 (for logic node) =-1 (for logic output node)
3	ts*	fanout schedule time
4	lval	logic value (3-bits for current value b2b1b0 3-bits for previous value b5b4b3 1=0, 2=1, 3=X)
5	lstr	logic strength (16-bits for current value 16-bits for previous value minimum strength = 1 ; maximum strength = 65,536)
8	modptr	1: capacitance at node 2: node decay delay value
7	dectim	node decay time

**ELECTRICAL NODE :**

offset	abbrev.	definition
0	fop	fanout pointer
1	fip	fanin pointer
2	type	= 2 (for electrical node) =-2 (for electrical output node)
3	ts*	fanout schedule time(last time or next time)
4	Vn-1	current node voltage
5	Vn-2	previous node voltage
6	capptrs	points to node capacitance values in rvals
7	tsn-1*	last time processed (associated with Vn-1)
8	tsn-2*	previous time processed (associated with Vn-2)

**VRAIL NODE :**

offset	abbrev.	definition
0	fop	-1 (not used)
1	fip	-1 (not used)
2	type	=5 for a vrail node
3	vn	current node voltage = constant
4	vn-1	previous node voltage = constant = vn

INTEGER information is typically accessed using the nodptr array

i.e.  $\text{info} = \text{imem}(\text{nodptr} + \text{locnod} + \text{ipos})$

**imem** : integer memory maintained by memory manager  
**nodptr** : node information data structure origin  
**locnod** : position of 1st piece of info for node  
**ipos** : position of desired info

REAL information is accessed through one more level of indirection:

i.e.  $\text{capacitance} = \text{rmem}(\text{rvals} + \text{imem}(\text{nodptr} + \text{locnod} + 5))$

**rmem** : real memory maintained by memory manager  
**rvals** : origin of real value array

- (2) **Fanin and Fanout Lists:** Fanin and fanout lists are stored with the node data structure. Fanins to a node are all elements which can affect the value of the node. Fanouts of a node are all elements which can be affected by a new value at the node. They are set up in the LOGFA, TIMFA and ENDFA sub-routines.

locfol:	0	unused location
	1	element 1 ptr
	2	element 2 ptr
	3	element 3 ptr
		.
		.
		.
	n	- element n ptr

If there is only one element in the fanin list (which is often the case), then this list does not exist. The fl pointer in the node data structure has a -ve sign to denote that it is the element pointer itself.

locfl:	0	schedular link
	1	element 1 ptr
	2	element 2 ptr
	3	element 3 ptr
		.
		.
		.
	n	- element n ptr

- (3) **Models:** SPLICE1 stores model information using two levels of indirection so that one model may be referenced by many elements.

model info pointers are stored in an array called mmdpnr:

mmdpnr:	0	locmod 0
	1	locmod 1
	2	locmod 2
	3	locmod 3
		.
		.
		.
	n	locmod n

locmod points into a table called modptr which is organized as follows:

modptr:	0	modtyp 1	(model type)
	1	locpar 1	(location of parameters)
	2	modtyp 2	
	3	locpar 2	
	4	modtyp 3	
	5	locpar 3	
		.	
		.	
		.	

locpar points into rvals which is an array of floating-point quantities and so parameters are accessed as follows:

$$\text{parameter} = \text{rmem} (\text{rvals} + \text{locpar})$$

The rvals array is just a set of real values in the rmem space.

rvals :	0	rvalue 0
	1	rvalue 1
	2	rvalue 2
	3	rvalue 3
		.
		.
		.
	n	rvalue n

- (4) **Elements:** Elements are initially written out to scratch files (timel, logel) by the routine SAVEL. Once they are read back in, they are stored in the array `elmptr` with the following format:

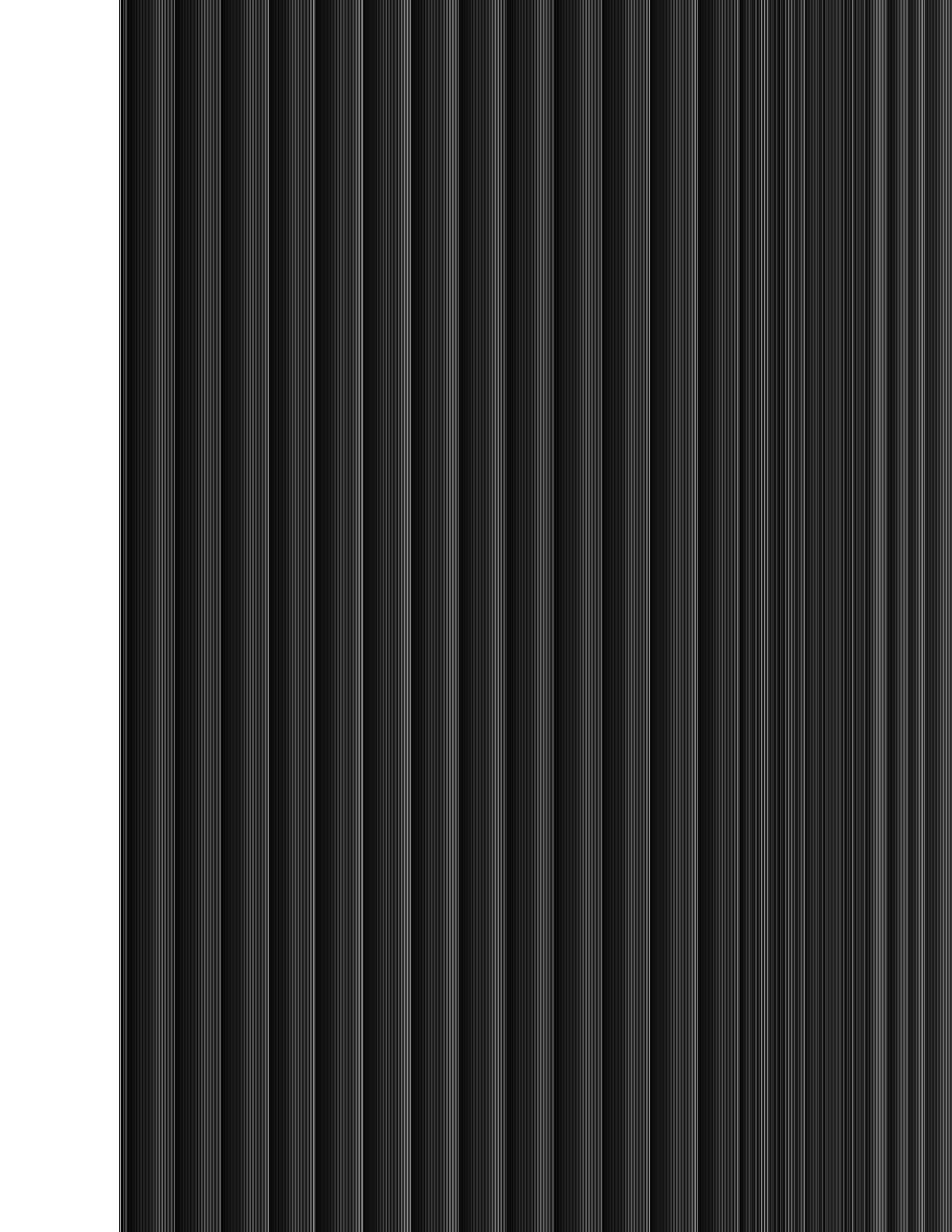
<code>elmptr :</code>	0	<code>-modnum</code>	(first logic element)
	1	<code>noutputs</code>	(number of outputs)
	2	<code>node1</code>	
	3	<code>node2</code>	
	4	<code>node3</code>	
		.	
		.	
		.	
	i	<code>-modnum</code>	(second logic element)
	i+1	<code>noutputs</code>	(number of outputs)
	i+2	<code>node1</code>	
	i+3	<code>node2</code>	
		.	
		.	
		.	
	<code>nlogwds+0</code>		(last logic element node)
	<code>nlogwds+1</code>	<code>-modnum</code>	(first electrical element)
	<code>nlogwds+2</code>	<code>noutputs</code>	(number of outputs)
	<code>nlogwds+3</code>	<code>node1</code>	
	<code>nlogwds+4</code>	<code>node2</code>	
		.	
		.	
		.	
	<code>ntimwds+0</code>		(last electrical node)

- (5) **Scheduler:** The time queue is made up of 2 - 100 word arrays and a pool for any events which do not fall within 200 timepoints of the beginning of the queue.

QUEUE 1		time
iscb1 :		0
		1
		2
	.	
	.	
lscb1 :		99

QUEUE 2		time
iscb2 :		0
		1
		2
	.	
	.	
lscb2 :		99

POOL	
iscb3 :	TIME 1
	LOCFOL 1
	TIME 2
	LOCFOL 2
	TIME 3
	LOCFOL 3
	.
	.
lscb3 :	-1



## **APPENDIX III**

### **SPLICE1.8 Electrical Element Model Equations**

---



## Electrical Element Model Equations

### 1. Resistors

$$G_{eq} = \frac{1}{R}$$

$$I_{eq} = \frac{(V_1 - V_2)}{R}$$

### 2. Floating Capacitors

$$G_{eq} = \frac{C_{float}}{h}$$

$$I_{eq} = C_{float} \frac{(V_1^n - V_1^{n-1}) - (V_2^n - V_2^{n-1})}{h}$$

### 3. Transistors

#### a. Triode Region

$$I_{eq} = \mu C_{ox} \frac{W}{L} (V_{gs} - V_T - \frac{V_{ds}}{2}) V_{ds} (1.0 + \lambda V_{ds})$$

#### Drain node

$$G_{eq} = \mu C_{ox} \frac{W}{L} ((V_{gs} - V_T - \frac{V_{ds}}{2}) V_{ds} \lambda + (1.0 + \lambda V_{ds}) (V_{gs} - V_T - V_{ds}))$$

#### Source Node

$$G_{eq} = \mu C_{ox} \frac{W}{L} ((V_{gs} - V_T + V_{ds} \frac{\gamma}{\sqrt{V_{sb} + 2\phi_F}}) (1.0 + \lambda V_{ds}) + (V_{gs} - V_T - \frac{V_{ds}}{2}) \lambda V_{ds})$$

#### b. Saturation Region

$$I_{eq} = \frac{\mu C_{ox}}{2} \frac{W}{L} (1.0 + \lambda V_{ds}) (V_{gs} - V_T)^2$$

**Drain Node**

$$G_{dq} = \frac{\mu C_{ox}}{2} \frac{W}{L} (V_{gs} - V_T)^2 \lambda$$

**Source Node**

$$G_{sq} = \frac{\mu C_{ox}}{2} \left( (V_{gs} - V_T)^2 \lambda + (V_{gs} - V_T) \left( 1.0 + \frac{\gamma}{\sqrt{V_{sb} + 2\phi_F}} \right) (1.0 + \lambda V_{ds}) \right)$$